NTNU
Norwegian University of
Science and Technology

# Online Voltage Stability Monitoring in Distribution Networks

Hans Kristian Hansen

Master of Science in Electric Power Engineering
Submission date: June 2017
Supervisor: Kjetil Uhlen, IEL

Norwegian University of Science and Technology
Department of Electric Power Engineering

# Preface

This thesis contributes the final work of the Master Programme Electric Power Engineering, at the Faculty of Information Technology and Electrical Engineering, at the Norwegian University of Science and Technology (NTNU). I would like to thank my supervisor, Professor Kjetil Uhlen, for valuable guidance and helpful insights during the work with my master's thesis. In addition, I would like to thank my co-supervisor, Postdoc Dinh Thuc Duong for interesting discussions and an enjoyable time at the smart grid laboratory doing some hands on work.

June 11, 2017, Trondheim

Hans Kristian Hansen

# Abstract

Power systems are often operated close to their stability limit. Line contingencies or other disturbances can cause the system to lose stability. If the power system loses stability counteractions have to be taken or else interruption in parts of, or in the whole system, occurs. In order to identify operational limits, the system operator needs the appropriate tools to make counteractions towards maintaining the security of operation.

Phasor measurement unit utilization has great potential for improved situational awareness in power system operation. This thesis assesses three indicators to monitor voltage stability in real time. All indicators are composed of changes in power with respect to changes in load. The indicators are based on local phasor measurements at the load bus, meaning no information about the topology is taken into account. In addition, two methods for estimating the Thevenin impedance and accordingly the maximum power transfer are reviewed. The methods and the indicators are suitable for online implementations to visualize the current state of the system and the distance to voltage instability.

Experiments realized through a laboratory power system consisted of a coil, a flexible line equivalent, a transformer and an adjustable resistive load. The scenarios the system was exposed to was an increase in load power demand and a line contingency. MATLAB simulations beforehand illustrate the theoretical behavior of the laboratory experiments.

As the indicators are able to detect the maximum power transfer limit, the trajectories visualizing the indicators will be of great benefit for the grid operators to identify the distance to the stability limit of the power system. As a large disturbance results in a severe change in power, the indicators need proper filtering depending on the desired monitoring. The estimation of the Thevenin impedance was validated and is corresponding with the calculated system impedance based on laboratory components. Nevertheless, the methods and indicators are viable for practical implementations in power systems to have an online voltage stability monitoring.

# Sammendrag

Kraftsystemer driftes ofte nær stabilitetsgrensen. Linjeutfall eller andre driftsforstyrrelser kan føre til at systemet mister stabiliteten. Hvis kraftsystemet mister stabilitet, må handlinger utføres for å unngå strømbrudd i deler av nettet, eller i nettets helhet. For å identifisere stabilitetsgrenser trenger systemoperatøren de riktige verktøyene for å gjøre tiltak som opprettholder kraftsystemet på en trygg måte.

Visermåleenheters (PMU) utnyttelse har et stort potensiale for å forbedre situasjonsforståelsen i drift av kraftsystemer. Denne avhandlingen vurderer tre indikatorer for å overvåke spenningsstabilitet i sann-tid. Alle indikatorer er sammensatt av endringer i effekt med hensyn på endringer i belastning. Indikatorene er basert på lokale visermålinger på last samleskinnen, noe som betyr at ingen informasjon om topologien er tatt i betraktning. I tillegg vurderes to metoder for estimering av Thevenin impedansen og maksimal kraftoverføring. Metodene og indikatorene passer for online implementeringer for å visualisere systemets nåværende tilstand.

Eksperimenter ble gjennomført ved hjelp av laboratoriets kraftsystem som besto av en spole, en fleksibel linjeekvivalent, en transformator og en justerbar resistiv belastning. Scenariene systemet ble utsatt for, var en gradvis økning i belastning og et linjeutfall. På forhånd ble det gjort MATLAB simuleringer for å illustrert den teoretiske oppførelsen av laboratorieforsøkene.

Siden indikatorene er i stand til å oppdage maksimal kraftoverføring under gradvis økt belastning, vil trendkurver som visualiserer indikatorene være en stor fordel for nettoperatørene for å identifisere avstanden til stabilitetsgrensen og vil øke situasjonsbevisstheten til nettoperatørene. Linjeutfallet forårsaker store endringer i effekt, det medfører at indikatorene må ha riktig filtrering avhengig av hvilke overvåkning en ønsker. Estimeringen av Thevenin impedansen er validert og korresponderte med den beregnede systemimpedansen basert på laboratoriekomponentene. Dette gjør det mulig å gi en tidlig varsel om spenningsinstabilitet, noe som er avgjørende for sikker og pålitelig drift.

# Contents

# List of Figures

# List of Tables

# Acronyms

**SCADA** Supervisory control and data acquisition

**PMU** Phasor measurement unit

**GPS** Global positioning systems

**PDC** Phasor data concentrators

**pu** per unit

**PV curve** Power-voltage characteristic

**ISI** Impedance stability index

**S-ZI** S-Z sensitivity indicator

**S-YI** S-Y sensitivity indicator

**NLI** New LIVES Index

**Hz** Hertz

# Chapter 1

# Introduction

## 1.1 Background and Objective

Voltage stability in power systems is one of the main concerns when it comes to operation. Depending on a specific operation situation, voltage instability can lead to a system collapse or blackout for many consumers. Faults in the system are often the cause of energy not supplied, and reasons for faults are often weather conditions and vegetation. These faults happen as chain reactions with little time to react, making system operation difficult.

The most common reason for power outages for Norwegian consumers are faults in the distribution network [3]. A fault in the distribution grid often leads to power line disconnects, sometimes the consequence is that the consumers are left without electric power supply.

The distribution network is no longer passive, in the future smart grid there will be requirements for coordination between the transmission and distribution networks in order to secure operation of the power system. Reinforcements on the grid are not always economically beneficial. Smart operation using measurements to monitor certain places in the grid, increasing predictability, is an absolute in the future. In this context, corrective actions can be taken at the distribution level to improve critical operation conditions in the power system. To have knowledge about the situation of the power system the operators need the correct tools.

Real-time indicators for voltage stability monitoring is one of the central tools to signify the margin to operational limits.

With this need for online monitoring tools for power system as motivation, this thesis utilizes PMU measurements to identify the voltage stability limit.

## 1.2 Scope of Work

In the work with this thesis, voltage stability indicators suitable for use in online applications are to be examined, together with the estimation of the Thevenin impedance of the system. Then, supported by local phasor measurements of voltage and current of the load, the maximum power transfer limit is estimated.

Experiments are done on a laboratory setup consisting of a coil, a flexible distribution line equivalent, a transformer and a load. Phasor measurements of voltage and current are performed by a PMU located at the load bus. The system will be subjected to events where the load demand gradually is increased, and the system impedance is increased, which is a result of disconnecting a feeder supplying power to the load.

The theoretical behavior of the power system is studied by using a simplified model created and the events performed in the laboratory are simulated in MATLAB.

Although power system stability is a many-sided phenomenon, the scope of this thesis is limited to the study of voltage stability.

## 1.3 Outline of Thesis

Chapter 1 presents an overview and motivation behind this thesis, as well as an introduction of the work that has been done. Chapter 2 presents terminology and definitions relevant to this report. Chapter 3 introduces the background theory of voltage stability, followed by Chapter 4

with descriptions and theory behind three selected voltage stability indicators and the estimation of the Thevenin impedance with the corresponding maximum power transfer limit. Chapter 5 presents the laboratory power system with its stationary components and its connections, before moving on to describe the MATLAB simulation and its parameters. Chapter 6 shows the experiment and simulation case descriptions, which also presents and discusses the obtained results. The conclusion is given in Chapter 7 together with ideas for further work.

# Chapter 2

# Power System Stability

The power system is dependent on some key features to achieve desired operation. When considering the situation of a power system there are some key properties and terminologies that should be known.

**Disturbances** are events that are accidental, and may result in extraordinary system operation, depending on the degree and situation.

**Contingency** is an unforeseen fault of one or more system components [4]. These may be generators, transformers, transmission lines or other electrical components.

**Security** is the ability of the power system to withstand sudden disturbances and its ability to resist disturbances since the risk after a contingency is a change of interruption of power to the customer connected to the grid.

Voltage stability is a subsection of power system stability as shown in Fig. 2.1. Voltage instability in a power system leads to an uncontrollable drop in system voltages as a result of a disturbance. The problem can spread to wider areas due to cascading reaction, stated as a voltage collapse.

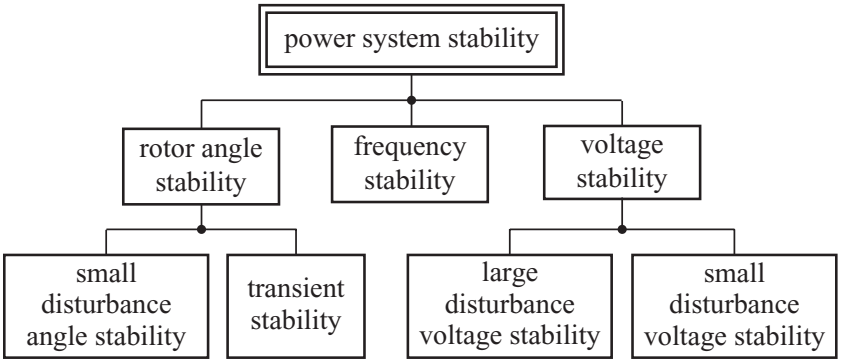


Figure 2.1: Classifications of power system stability [1].

## 2.1 Definition of Voltage Stability

The definition of voltage stability is given by The IEEE/CIGRE Join Task Force [5]. "Voltage stability is the ability of a power system to maintain steady, acceptable voltages at all buses in the system under normal operating conditions and after being subjected to a disturbance." Further voltage stability is categorized into the following subcategories.

**Small disturbance** voltage stability is concerned with the system´s ability to control voltages following incremental changes in system load. The small changes in the system are typically regular changes in load.

**Large disturbance** voltage stability is concerned with the system´s ability to control voltages after contingencies. Large disturbances can last from seconds to hours depending on the repair time, and may result in voltage collapse for a part of or the whole grid. It is a nonlinear process and cannot be analyzed using linearizing methods.

Voltage stability is determined in both cases as the ability of the system to maintain a steady voltage after a change in the system [6].

## 2.2 Phasor Measurement Unit

A phasor is a time-independent method of describing the magnitude of the sinusoidal signal and its angle based on the angular difference between a chosen reference time and the amplitude of the sinusoid. The definition of a phasor is closely associated with the representation of a periodic waveform as a rotating vector [1]. This is illustrated in Fig. 2.2, a vector $\vec{V}_m$ is rotating with angular speed $\omega$ with respect to a stationary reference axis. The position of the vector is given by

$$\vec{V}(t) = V_m e^{j(\omega t+\delta)} \tag{2.1}$$

where $V_m$ is the amplitude and $\delta$ is the phase shift with respect to the reference frame ($Re$). Projection of $\vec{V}(t)$ on the horizontal axis is periodically time domain, given as

$$v(t) = V_m \cos(\omega t + \delta) \tag{2.2}$$

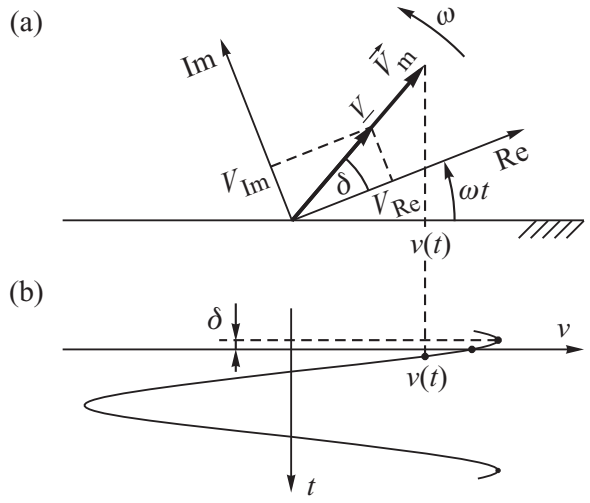


Figure 2.2: (a) Rotating vector. (b) Corresponding time-domain signal [1].

Phasor measurement unit (PMU) is a measurement device that takes in voltage and current measurements. All the measurements are given a time stamp obtained from clocks synchronized using global positioning systems (GPS) [7].

The benefits of PMUs compared to the conventional supervisory control and data acquisition (SCADA) systems, is the data acquiring rate that increases the situational knowledge. Traditional SCADA systems acquire data every 3-10 seconds, and PMUs acquire data up to 60 times per second [8], meaning PMU measurements has potential to observe the faster dynamic phenomena occurring in a power system. Fig. 2.3 illustrates two differently located substations, A and B. While Fig. 2.4a shows how measurements from substation A and B can be obtained and time-stamped. The time-stamped data is sent to phasor data concentrators (PDC) so a power flow can be obtained by combining the measurements. Fig. 2.4b illustrates output signals of the PDC from substation A and B.

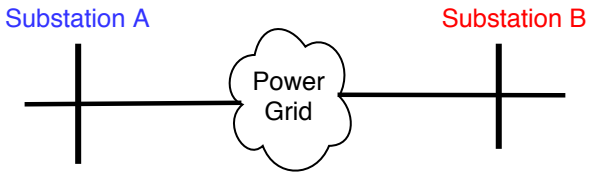


Figure 2.3: Substation A and B.

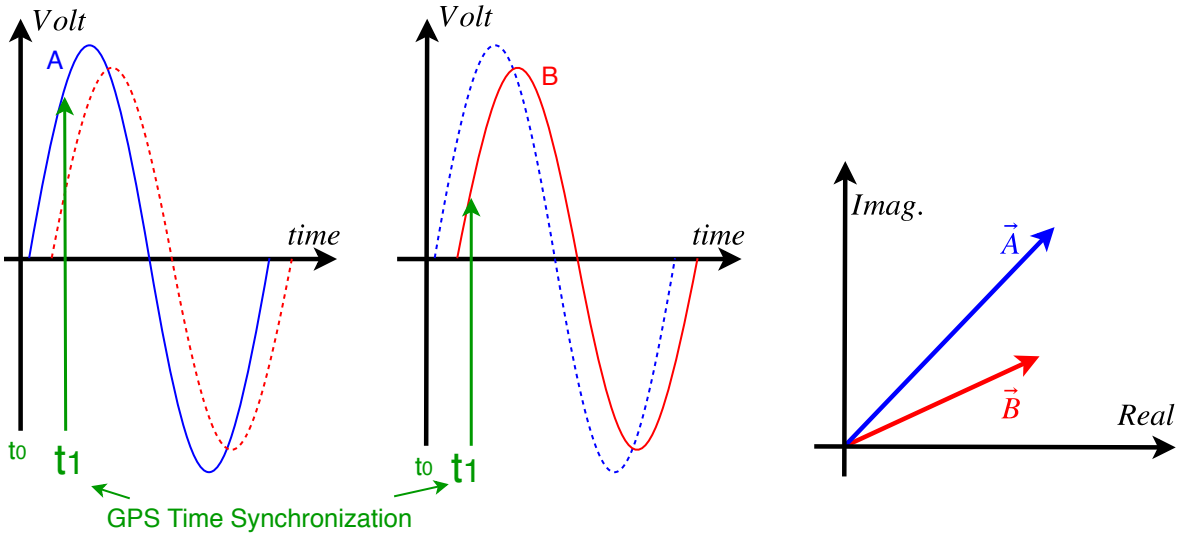


(a) Data collection of PMU.

(b) Output signals from PDC at $t = t_1$.

Figure 2.4: Time domain and phasors illustation [2].

# Chapter 3

# Key Aspects of Voltage Instability

## 3.1 Max Loadability

Voltage instability is in general, a consequence of a load response to a disturbance that will exceed the maximum power transfer limit. To highlight the maximum power transfer limit in a power system, consider a simple two-bus system represented in Fig. 3.1. An equivalent voltage source $E$ set as the reference with an angle equal to zero, behind a line reactance $X$. The resistances of the generator and the transmission line are neglected. Voltage $V$ has an angle $\delta$, and $I$ is the current drawn by the load, with the power factor angle $\varphi$. The load is shown as a real and reactive power $P + jQ$.

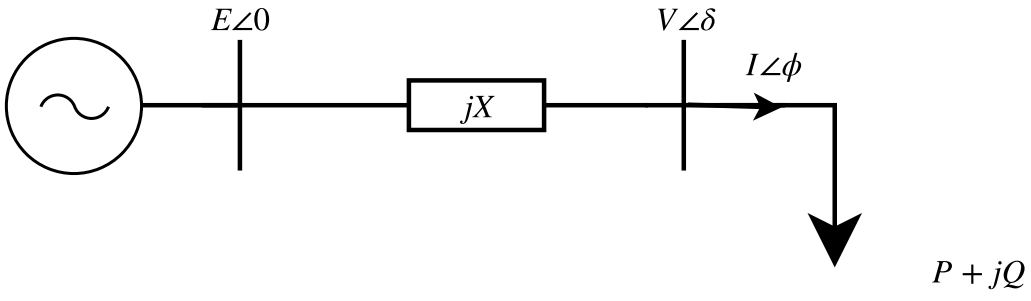


Figure 3.1: Simple two-bus system.

The real and reactive power can be calculated by

$$P = V I \cos\varphi = \frac{EV}{X}\sin\delta \tag{3.1}$$

$$Q = V I \sin\varphi = \frac{EV}{X}\cos\delta - \frac{V^2}{X} \tag{3.2}$$

Combining (3.1) and (3.2), including a trigonometric identity $\sin^2\delta + \cos^2\delta = 1$, the expression can be written as

$$\left(\frac{EV}{X}\right)^2 = P^2 + \left(Q - \frac{V^2}{X}\right)^2 \tag{3.3}$$

Rewriting (3.3) and solving with respect to $V^2$

$$(V^2)^2 + (2XQ - E^2)V^2 + X^2(P^2 + Q^2) = 0 \tag{3.4}$$

(3.4) is a quadratic equation with two solutions. By including $Q = P\tan\varphi$, and solving it with a constant power factor [1]. Expressing the voltage and power in per unit (pu) quantities $v = \frac{V}{E}$ and $p = \frac{PX}{E^2}$ the solutions are

$$u = \sqrt{\frac{1}{2} - p\tan\varphi \pm \sqrt{\frac{1}{4} - p^2 - p\tan\varphi}} \tag{3.5}$$

Based on (3.5), a power-voltage characteristic (PV curve) can be drawn. In Fig. 3.2 PV curves with various power factors are shown. From fundamental circuit theory it is known that the maximum power transfer limit is reached when the magnitude of the load impedance is equal the magnitude of the system impedance. There are two solutions for all other power levels on the curve, one at the upper part of the curve and one at the lower part. The upper part of the curve (higher voltage solution) is the normal and stable mode of operation.

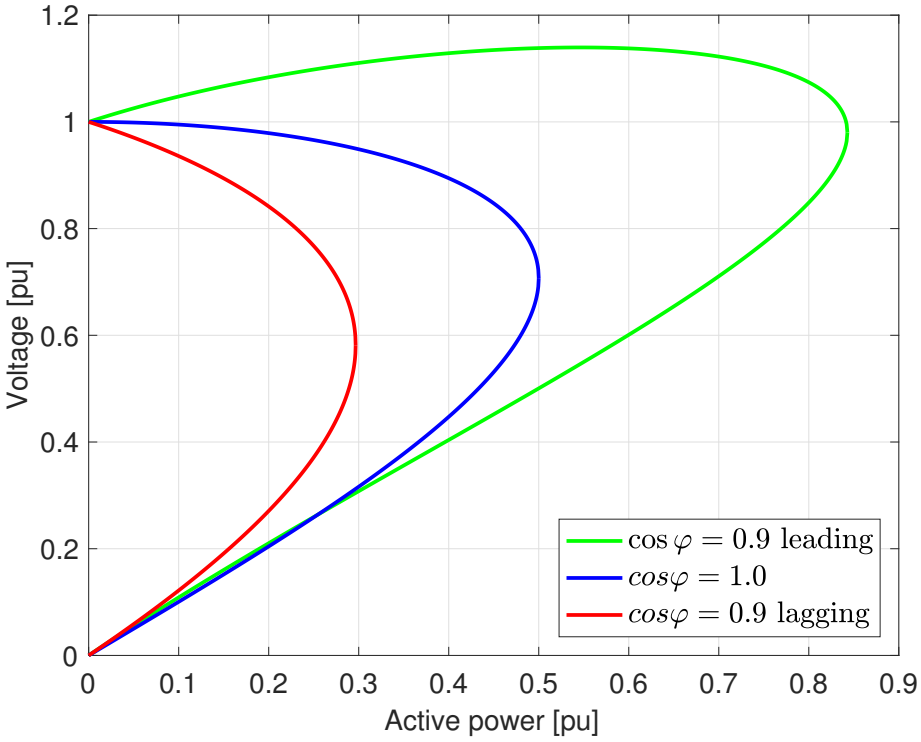


Figure 3.2: PV curves with different power factor angles.

The PV curve is useful to determine the difference between the current load and the maximum load. It is possible to find the maximum load which is the critical point and can also be related to the "nose" point of the PV curve. This condition is fulfilled when the inner root of (3.5) is zero. At this point there is only one solution for the voltage [9]. Maximum power can then be expressed by normalized values

$$p_{max} = \frac{1 - \sin\varphi}{2\cos\varphi} \tag{3.6}$$

If the load increases, the voltage follows accordingly depending on the power factor of the load. The load can increase until it reaches the nose point, this is where the grid cannot supply any more power to the load. If the load continuous to increase, the voltage will drop accordingly again depending on the power factor of the load. The maximum power point is the critical point.

At overcompensated loads ($\tan\varphi < 0$), the voltage will increase as the power rises and could be reaching the maximum power limit at nominal voltage. This makes the voltage magnitude a bad indicator for voltage stability evaluation [10].

## 3.2 Influence of the Load modelling

The word load can have several meanings in power system engineering, in general it could be seen as a device connected to the power system that consumes power. Static loads will have different behaviors depending on the type. After a disturbance the system may provide lower voltages, and since most loads are voltage dependent the power also lowers. As a result of the disturbance, the load also tries to restore its power to pre-disturbance power, which may increase the stress on the already weakened grid. This is characterized as load restoration [11].

Depending on the characteristics there are different types of modeling. PQ-loads are the easiest way to model a load, they consist of a constant power component which is independent of the voltage applied, this model is often used in load flow computations. The PV curve shown in Fig. 3.3b illustrates that the change in power is independent of the voltage.

ZIP-load is modeled as a polynomial load [9]. The voltage characteristic contains the sum of constant impedance ($Z$), constant current ($I$) and constant power($P$) relations. The active and reactive power are modeled as functions of voltage

$$P = P_0 \left[ a_1 \left( \frac{V}{V_0} \right)^2 + a_2 \left( \frac{V}{V_0} \right) + a_3 \right] \tag{3.7}$$

$$Q = Q_0 \left[ a_4 \left( \frac{V}{V_0} \right)^2 + a_5 \left( \frac{V}{V_0} \right) + a_6 \right] \tag{3.8}$$

The relation is weighted so that

$$a_{1,4} + a_{2,5} + a_{3,6} = 1 \tag{3.9}$$

The result of having the power demand depend on the voltage is illustrated in Fig. 3.3a.

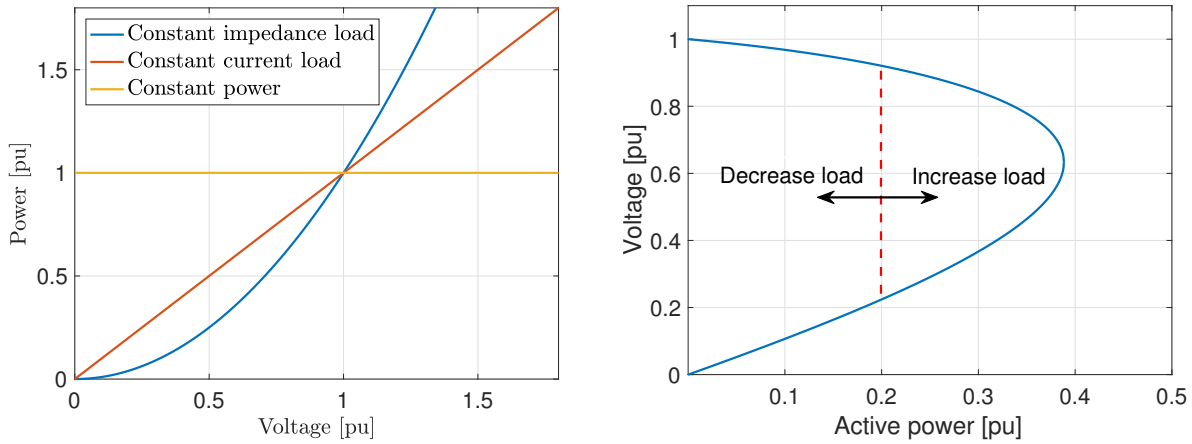


(a) Power versus voltage.

(b) PQ load PV curve.

Figure 3.3: Load modelling and load voltage dependency.

A PV curve for a typical ZIP load for a given operation point is shown in Fig. 3.4, it can be seen that when increasing the load, the nose point is reached. If the load is increased even more, the actual power is decreasing.

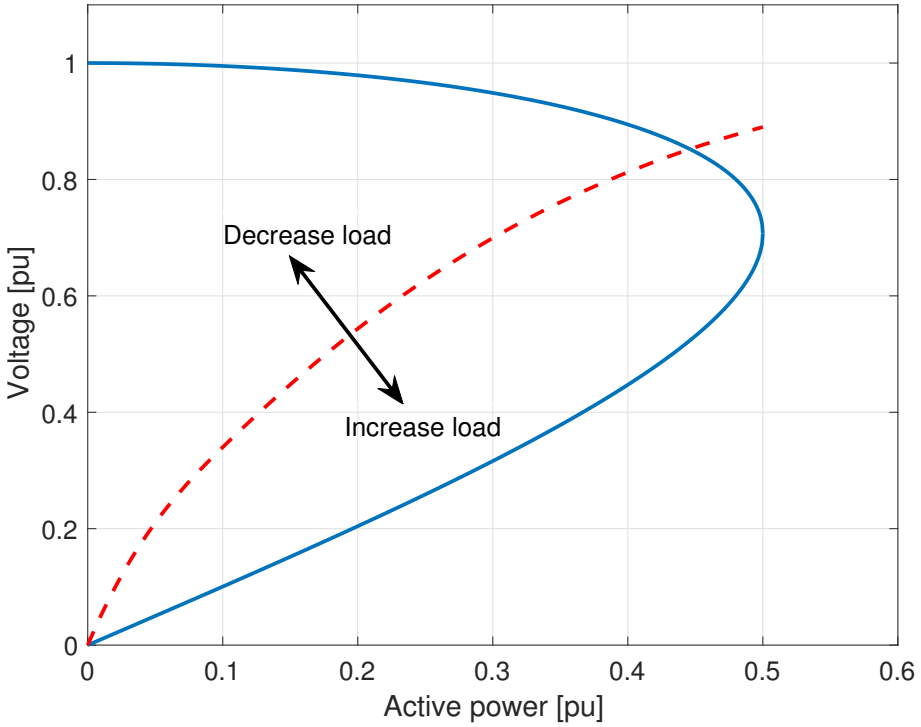


Figure 3.4: Typical ZIP load characteristic.

## 3.3 Change in Network Topology

One of the most common situations for voltage stability issues is when the network is being weakened, for example by the outage of a power line [9]. The case can be studied using (3.5) from Section 3.1. In actual values, the voltage can be expressed by

$$V = \sqrt{\frac{E^2}{2} - XQ \pm \sqrt{\frac{E^4}{4} - X^2P^2 - XE^2Q}} \tag{3.10}$$

By assuming only active power in the load demand, the equation can be reduced to

$$V = \sqrt{\frac{E^2}{V} \pm \sqrt{\frac{E^4}{4} - X^2P^2}} \tag{3.11}$$

Maximum power is when there is only one solution, also known as the nose point of the PV curve. This happens when the inner root equals 0, then we get

$$\frac{E^4}{4} - X^2P^2 = 0 \tag{3.12}$$

Sorting with respect to the active power gives

$$P = \frac{E^2}{2X} \tag{3.13}$$

The case of a line contingency can be set up and studied, in Fig. 3.5 a line contingency is illustrated.

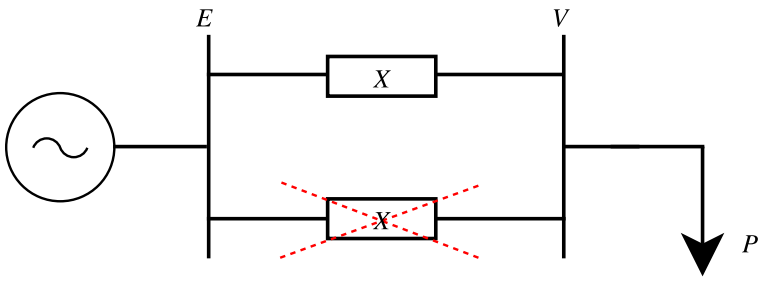


Figure 3.5: Line contingency principle.

Before the contingency occurs the reactance of the lines is in parallel, meaning the total reactance is $X/2$. After the contingency the reactance is $X$, meaning the reactance has doubled. Examining (3.13), shows that the maximum power limit is cut to half of the original value because of the line contingency. Fig. 3.6 demonstrates the effect of a line outage with a PV curve.

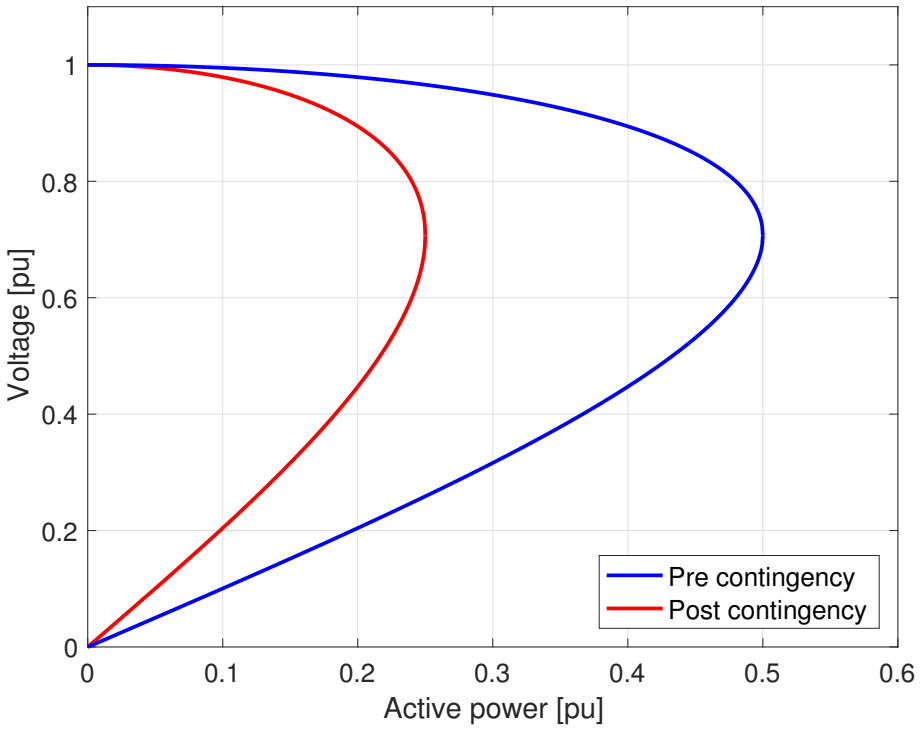


Figure 3.6: PV curve before and after a line outage.

# Chapter 4

# Online Voltage Stability Monitoring

This chapter presents the Thevenin impedance seen at the load bus and three selected indicators for online voltage stability monitoring are presented. The Thevenin impedance and indicators are able to continuously assess the current situation of the power system and are based on local measurements taken by a PMU located at the load bus, meaning network topology is not taken into account. The presented indicators are based on following

- The derivative of apparent power of the load with respect to the magnitude of its impedance.
- The derivative of apparent power of the load with respect to the magnitude of its admittance.
- The derivative of active power of the load with respect to its conductance.

## 4.1 Thevenin Equivalent

By considering the classic Thevenin equivalent seen from the load bus [12]. The Thevenin equivalent circuit is shown in Fig. 4.1 consists of a Thevenin voltage source $\vec{E}_{Th}$ behind the Thevenin impedance $\vec{Z}_{Th}$. The load is considered as the impedance $\vec{Z}_L$. The reference phasor is the voltage source $\vec{E}_{Th}$, hence the phase angle is equal to zero, $\vec{E}_{Th} = E_{Th}\angle 0$. The local measurements of voltage $\vec{V}$ and current $\vec{I}$ are located at the load bus.

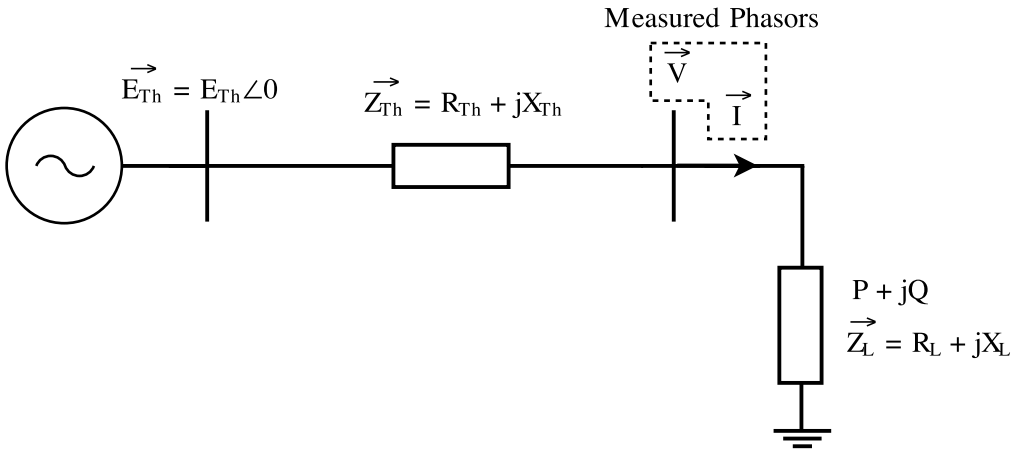


Figure 4.1: Thevenin equvialent circuit.

Voltage stability is directly connected to the relationship between the load impedance and the Thevenin impedance, with the corresponding maximum power limit. The method is a way of estimating the strength of the power system connected to the bus and comparing this estimated Thevenin impedance with the actual value of the load. The closer the load demand is to the estimated load impedance magnitude, the more likely it is to have voltage stability issues. This indicator is called Impedance stability index (ISI) [13]. As long as the load impedance is larger than the Thevenin impedance the system is considered as stable. See Fig. 4.2 for an illustration.

$$ISI = \frac{|\vec{Z}_{Th}|}{|\vec{Z}_L|} \leq 1 \tag{4.1}$$

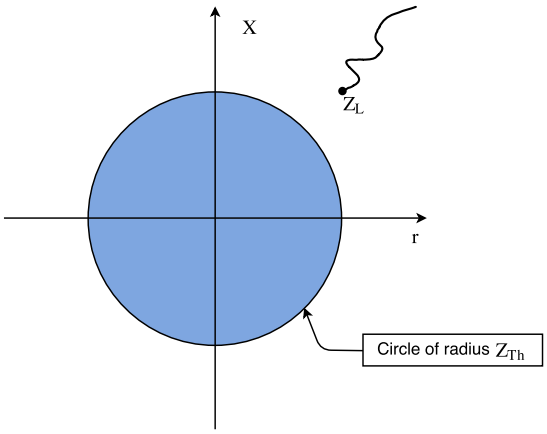


Figure 4.2: Relationship between the load impedance and the Thevenin impedance.

When the Thevenin impedance is known, the Thevenin voltage can be calculated by

$$\vec{E}_{Th} = \vec{V} + \vec{I}\vec{Z}_{Th} \tag{4.2}$$

Given the Thevenin equivalent, it is possible to estimate the maximum power transfer, $S_{Max}$, by assuming that the Thevenin impedance is equal to the magnitude of the load, $|Z_{Th}| = |Z_L|$. This results in [14]

$$S_{Max} = \frac{E_{Th}^2 \Big[ Z_{Th} - \big( Im(\vec{Z_{Th}}) \sin\varphi + Re(\vec{Z_{Th}}) \cos\varphi \big) \Big]}{2 \Big[ Im(\vec{Z_{Th}}) \cos\varphi - Re(\vec{Z_{Th}}) \sin\varphi \Big]^2} \tag{4.3}$$

After crossing the maximum loadability, voltage collapse can occur, differing on the load characteristics. The loads can be nonlinear and dynamic with a load recovery characteristic. Power system operation larger than the loadability limit is not predictable. It is reasonable to consider the maximum power transfer as the limit for voltage stability. Defining the power margin as the remaining power to be drawn from a load as [14]

$$S_{Margin} = \frac{S_{Max} - S_L}{S_L} \cdot 100\% \tag{4.4}$$

where $S_L$ is the apparent load power.

## 4.2 Thevenin Impedance Phase Angle

The ratio $X_{Th}/R_{Th}$ is not calculated beforehand, and the ratio has an effect on the estimated Thevenin impedance. Defining the angle of the Thevenin impedance as

$$\tan^{-1} \frac{X_{Th}}{R_{Th}} = \alpha \tag{4.5}$$

$\alpha$ is an element in the angle $\theta$, which is the angle between $\vec{Z}_L$ and $\vec{Z}_{Th}$, Fig. 4.3 illustrates the impedances with corresponding angles. The angle is a setting parameter and can be adjusted to the typical $X/R$ ratio of the power lines in the studied area. An incorrect ratio can lead to a large error in the estimation of the Thevenin impedance [10].

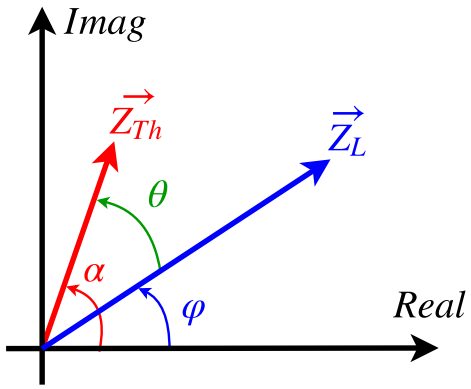


Figure 4.3: Angle $\theta$, between the load impedance and the Thevenin impedance.

## 4.3 S-Z Method

An approach to estimating the Thevenin impedance is developed in reference [10]. The method proposes an algorithm to estimate the Thevenin impedance seen from the load bus based on S-Z sensitivity. Measurements required are the voltage and current phasors. The S-Z sensitivity indicator is created based on the derivative of apparent load power with respect to the load impedance. The indicator can detect the maximum loadability, which is linked with voltage stability as described in Section 3.1.

### 4.3.1 Estimation of the Thevenin Impedance

Chapter 4.1 presented the Thevenin equivalent of the system seen from a specific load bus. With the Thevenin equivalent in mind, the current can be expressed by

$$I = \frac{E_{Th}}{Z_{Th} + Z_L} = \frac{E_{Th}}{\sqrt{(R_L + R_{Th})^2 + (X_L + X_{Th})^2}} \tag{4.6}$$

By completing the square

$$(R_L + R_{Th})^2 + (X_L + X_{Th})^2 = Z_{Th}^2 + Z_L^2 + 2(R_L R_{Th} + X_L X_{Th}) \tag{4.7}$$

$Z_L$ and $Z_{Th}$ are the magnitude of the load and the Thevenin impedance, and $R_L R_{Th} + X_L X_{Th}$

is the scalar product of $Z_L$ and $Z_{Th}$,and $\theta$ is the angle between the Thevenin and the load impedance, by these assumptions the relation is

$$R_L R_{Th} + X_L X_{Th} = Z_L Z_{Th} \cos\theta \tag{4.8}$$

By combining (4.7) and (4.8) into (4.6) it gets

$$I = \frac{E_{Th}}{\sqrt{Z_{Th}^2 + Z_L^2 + 2Z_L Z_{Th}\cos\theta}} \tag{4.9}$$

The apparent load power can be expressed accordingly to

$$S_L = I^2 Z_L = \frac{E_{Th}^2 Z_L}{Z_{Th}^2 + Z_L^2 + 2Z_L Z_{Th}\cos\theta} \tag{4.10}$$

It is realistic to assume that Thevenin voltage $E_{Th}$ and impedance $Z_{Th}$ are constant for a short duration of time [10]. From (4.10) it is possible to derive the apparent power with respect to the load impedance magnitude

$$\frac{dS_L}{dZ_L} = \frac{E_{Th}^2 (Z_{Th}^2 - Z_L^2)}{(Z_{Th}^2 + Z_L^2 + 2Z_L Z_{Th}\cos\theta)^2} \tag{4.11}$$

By using (4.6) into (4.11) leads to

$$\frac{dS_L}{dZ_L} = \frac{I^2 (Z_{Th}^2 - Z_L^2)}{Z_{Th}^2 + Z_L^2 + 2Z_L Z_{Th}\cos\theta} \tag{4.12}$$

Defining

$$\zeta = \frac{dS_L}{dZ_L} = \frac{S_L^2 - S_L^1}{Z_L^2 - Z_L^1} \tag{4.13}$$

where

- $S_L^1$ and $Z_L^1$ are the load apparent power and load impedance at the start of change.
- $S_L^2$ and $Z_L^2$ are the load apparent power and load impedance at the end of change.

Inserting (4.13) into (4.12) and turning around to consider the Thevenin impedance $Z_{Th}$ as an unknown

$$(I^2-\zeta)Z_{Th}^2-2\zeta\cos\theta Z_L Z_{Th}-Z_L^2(I^2+\zeta)=0 \tag{4.14}$$

With this in mind, it is possible to find the Thevenin impedance $Z_{Th}$ with only phasor measurements of the voltage and current at a particular load bus. With the whole approach based on consecutive measurements within the variation of the apparent power and load impedance. The Thevenin impedance must be a real and positive number [10].

### 4.3.2 S-Z Sensitivity Indicator

Section 3.1 presented that the PV curve can be used to find the maximum power limit. Figure 3.2 shows that in the upper section of the curve the demand can be met if the load increases, but in the lower section the response is opposite. The variations of the load impedance ($dZ_L$) represents the demand, and the variations of apparent load power ($dS_L$) represents the response of the grid. The indicator is called S-Z sensitivity indicator (S-ZI) [10].

$$S-ZI=\frac{dS_L}{dZ_L} \tag{4.15}$$

It is important to understand the outcome of (4.15). Now consider the load impedance to decrease ($dZ_L<0$), and the S-ZI outcome will be determined by

- $S-ZI<0$ Power increases, the grid is able to meet the demand of the load. The load impedance is larger than the Thevenin impedance and is corresponding to the upper part of the PV curve.
- $S-ZI>0$ Power decreases, the grid does not meet the load demand meaning the load has passed the maximum load limit. The load impedance is smaller than the Thevenin impedance and corresponds to the lower part of the PV curve.
- $S-ZI=0$ Power is unchanged, meaning the maximum loadability limit is reached and is at the nose point of the PV curve. This happens when the load impedance is equal to the Thevenin impedance and corresponds to the nose point of the PV curve.

Considering (4.12), the relation between the magnitudes of the Thevenin impedance and the load impedance determines the sign of the S-ZI as follows

- $Z_L > Z_{Th} \leftrightarrow S - ZI < 0$ Magnitude of the load impedance is larger than the Thevenin impedance, the maximum loadability limit has not been reached.
- $Z_L < Z_{Th} \leftrightarrow S - ZI > 0$ Magnitude of the load impedance is smaller than the Thevenin impedance, the maximum loadability limit has been reached.
- $Z_L = Z_{Th} \leftrightarrow S - ZI = 0$ Magnitude of the load impedance is equal the Thevenin impedance, the load is reaching maximum loadability limit.

With (4.11) it is possible to draw a trajectory of the S-ZI with respect to the load impedance [10]. Based on a Norwegian distribution system the parameters are set to $E_{Th} = 19kV$ and the transmission lines set to a $X/R$ ratio equal 3. Fig. 4.4 shows the trajectories of the S-ZI with respect to the load impedance magnitude. The curves can be compared and have the same particular characteristic. When the load impedance is high (low demand) the S-ZI have the same trajectories for all Thevenin impedances. When the load is approaching maximum power transfer the curves flow away from each other. Fig. 4.5 magnifies where the S-ZI has its zero crossing. Regarding voltage stability, the curves for maximum loadability is reached when load impedance is equal to the Thevenin impedance.

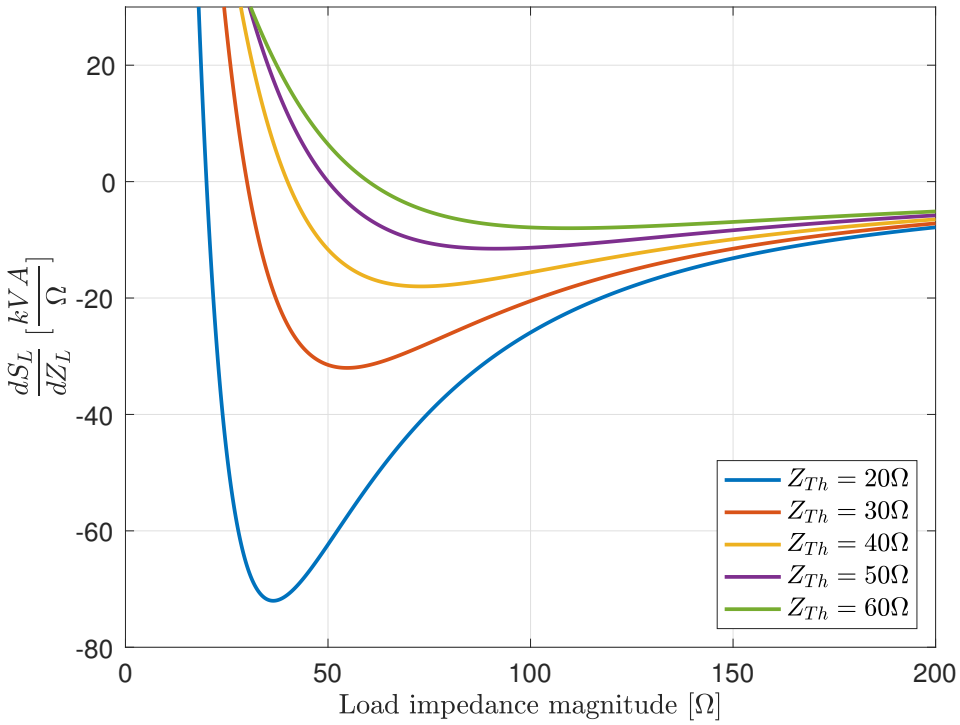


Figure 4.4: Trajectories of the S-ZI.

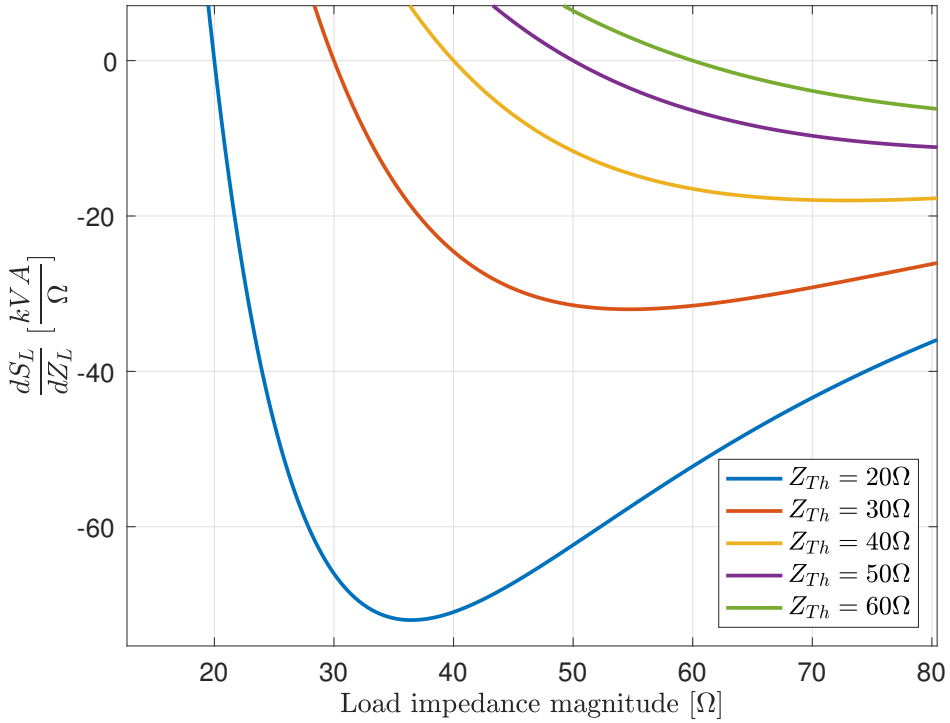


Figure 4.5: Magnified trajectories of the S-ZI.

## 4.4 S-Y Method

An approach to measure the stability margin is represented in [15]. The method is based on local measurements and on reducing the power system to a Thevenin equivalent. By doing the same approach as in Section 4.3 it is possible to estimate the Thevenin impedance seen from the load bus based on S-Y sensitivity. Measurements required are the voltage and current phasors. S-Y sensitivity indicator (S-YI) is created based on the derivative of apparent load power with respect to the load admittance. The indicator is also able to detect the maximum loadability.

### 4.4.1 Estimation of the Thevenin Impedance

Based on Fig. 4.1, the current was in (4.9) expressed by

$$I = \frac{E_{Th}}{\sqrt{Z_{Th}^2 + Z_L^2 + 2Z_L Z_{Th}\cos\theta}} \tag{4.16}$$

By substituting Ohms law into (4.16) an expression for the voltage at the load bus is given by

$$V = \frac{E_{Th} Z_L}{\sqrt{Z_L^2 + Z_{Th}^2 + 2 Z_L Z_{Th} \cos\theta}} \tag{4.17}$$

The load admittance, $Y_L$, is given by the inverse of the load impedance

$$Y_L = \frac{1}{Z_L} \tag{4.18}$$

Apparent power in (4.10) was

$$S_L = \frac{E_{Th}^2 Z_L}{Z_{Th}^2 + Z_L^2 + 2 Z_L Z_{Th} \cos\theta} \tag{4.19}$$

By inserting (4.18) into (4.19) it gets

$$S_L = \frac{E_{Th}^2 Y_L}{1 + Z_{Th}^2 Y_L^2 + 2 Y_L Z_{Th} \cos\theta} \tag{4.20}$$

From (4.20) it is possible to derive the apparent power with respect to the load admittance magnitude.

$$\frac{dS_L}{dY_L} = \frac{E_{Th}^2 (1 - Z_{Th}^2 Y_L^2)}{(1 + Z_{Th}^2 Y_L^2 + 2 Z_{Th} Y_L \cos\theta)^2} \tag{4.21}$$

Substituting $E_{Th}$ in (4.17) leads to

$$\frac{dS_L}{dY_L} = \frac{V^2 (1 - Z_{Th}^2 Y_L^2)}{1 + Z_{Th}^2 Y_L^2 + 2 Z_{Th} Y_L \cos\theta} \tag{4.22}$$

Defining

$$\xi = \frac{dS_L}{dY_L} = \frac{S_L^2 - S_L^1}{Y_L^2 - Y_L^1} \tag{4.23}$$

where

- $S_L^1$ and $Y_L^1$ are the load apparent power and load admittance at the start of change.
- $S_L^2$ and $Y_L^2$ are the load apparent power and load admittance at the end of change.

Turned around to consider the Thevenin impedance $Z_{Th}$ as an unknown

$$(\xi Y_L^2 + V^2 Y_L^2) Z_{Th}^2 + 2\xi Y_L \cos\theta Z_{Th} + (\xi - V^2) = 0 \tag{4.24}$$

With this in mind, it is possible to find the Thevenin impedance $Z_{Th}$ with only phasor measurements of the voltage and current at a load bus, with the whole approach based on consecutive measurements within the variations of the apparent power and load admittance.

### 4.4.2 S-Y Sensitivity Indicator

The deviation of the load admittance ($dY_L$) represents the demand, and the deviation of apparent power of the load ($dSL$) represents the response of the grid. The indicator is called S-Y sensitivity indicator (S-YI).

$$S-YI = \frac{dS_L}{dY_L} \tag{4.25}$$

Considering the outcome of this equation, let the load demand increase ($dY_L > 0$)

- $S-YI > 0$ The power increases, $dS_L$ is positive and the grid meets the demand, the load has not reached the point of maximum power transfer at the PV curve and is able to transfer more power.
- $S-YI < 0$ The power decreases, $dS_L$ is negative and the grid is not able to meet the demand, the load has crossed the point of maximum power transfer and is at the lower part of the PV curve.
- $S-YI = 0$ The power is unchanged, $dS_L = 0$, the maximum power transfer is reached and the grid is not able to transfter more power. This is equivalent to the nose point of the PV curve.

It is possible to look at the system as an admittance

$$Y_{Th} = \frac{1}{Z_{Th}} \tag{4.26}$$

Considering (4.22), the relation between the magnitudes of the Thevenin admittance and the load admittance determines the sign of the S-YI as follows

- $Y_L < Y_{Th} \leftrightarrow S - YI > 0$ Magnitude of the load admittance is smaller than the Thevenin admittance, the maximum loadability limit has not been reached.
- $Y_L > Y_{Th} \leftrightarrow S - YI < 0$ Magnitude of the load admittance is larger than the Thevenin admittance, the maximum loadability limit has been reached.
- $Y_L = Y_{Th} \leftrightarrow S - YI = 0$ Magnitude of the load admittance is equal the Thevenin admittance, the load is reaching maximum loadability limit.

With (4.21) it is possible to draw a trajectory of the S-YI with respect to the load admittance. By using the same parameters as in Section 4.3, $E_{Th}$ is set equal 19kV and the transmission lines $X/R$ ratio equal 3. Fig. 4.6 shows the trajectories of the S-YI with respect to the load admittance magnitude. Regarding voltage stability, the maximum loadability is crossed when load admittance is larger than the Thevenin admittance. This agrees well with the S-YI outcome listed previously.

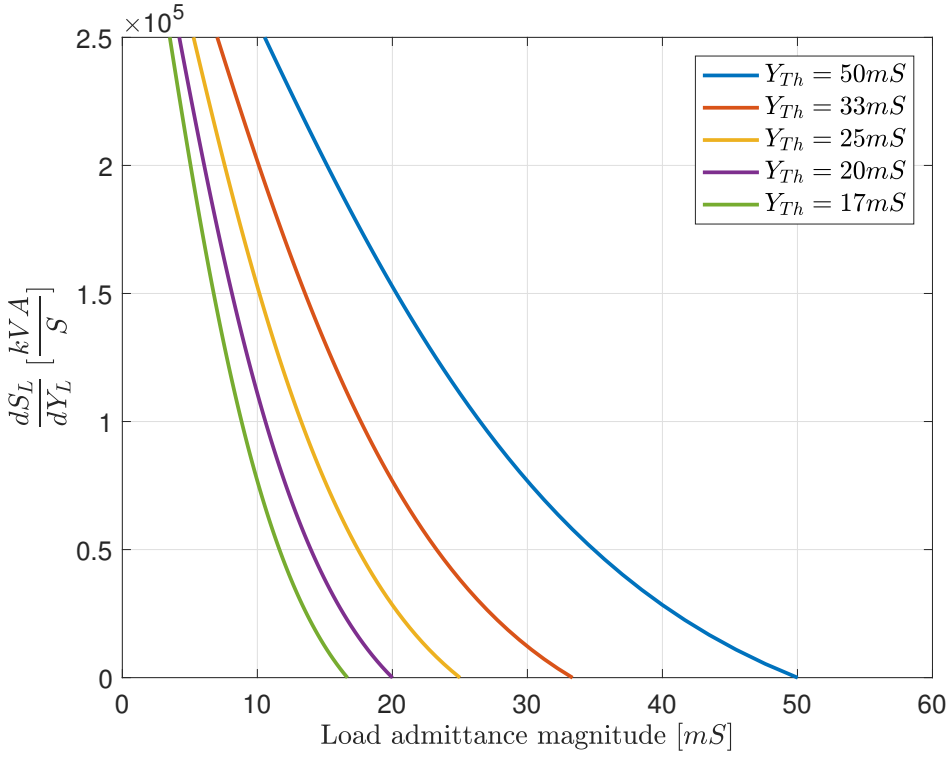


Figure 4.6: Trajectories of the S-Y sensitivity indicator.

## 4.5 Validating the Thevenin Impedance

The ratio can be identified using the ratio of $X/R$ of the lines in the study area, adjusting appropriately by comparing the trajectory of the S-Z or S-Y sensitivity indicators. If the $X_{Th}/R_{Th}$ ratio is incorrect, the operation point will not appear on the trajectory line, it is then possible to adjust the ratio until it is located on the trajectory line [10].

By comparing the indicator obtained from measurements with the trajectory drawn from the estimated Thevenin impedance, the Thevenin impedance can be validated. Fig. (4.7) shows a trajectory drawn with a computed Thevenin impedance and an actual value of the S-Y sensitivity and load. The operation point is not located on the trajectory, meaning the $X/R$ ratio needs corrections.

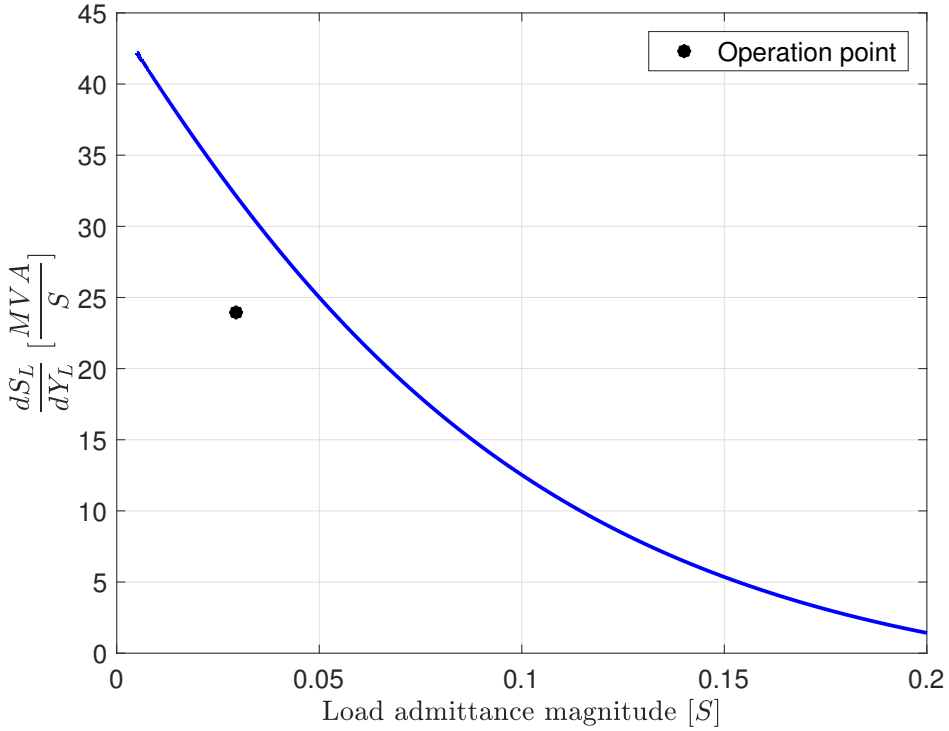


Figure 4.7: S-YI with an invalid operation point.

## 4.6 New LIVES Index

Centralized monitoring could in principle be possible if PMU´s were presented in every busbar in the power system, this is not yet a realistic option. Reference [16] presents an index based on changes in measured power and changes in apparent conductance seen from a transmission bus. In this report, the New LIVES Index (NLI) is studied with PMU measurements at the load bus.

The proposition is when an increase in load conductance allows more active power to flow, the monitored transmission bus is considered stable. On the other hand, when the system fails to deliver active power when the conductance increases, the system is then considered unstable in terms of voltage stability.

Considering the simplified two-bus system shown in Fig. 4.8, where the load is represented as an impedance behind a voltage source $\vec{E_{Th}}$, in series with an impedance $\vec{Z_{Th}}$. The admittance is

$$Y_L = G_L - jB_L \tag{4.27}$$

$$B_L = G_L \tan\varphi \tag{4.28}$$

By defining $\beta = \tan\varphi$, where $\varphi$ is the power factor angle. The admittance can be expressed by

$$Y_L = G_L(1 - j\beta) \tag{4.29}$$

The load can be represented as an admittance, where $G_L$ is the conductance of the load. The maximum power transfer and stability limit are both encountered when the impedance matching condition holds as described in Section 4.1.

$$Z_L = \frac{1}{G_L(1 - j\beta)} \tag{4.30}$$

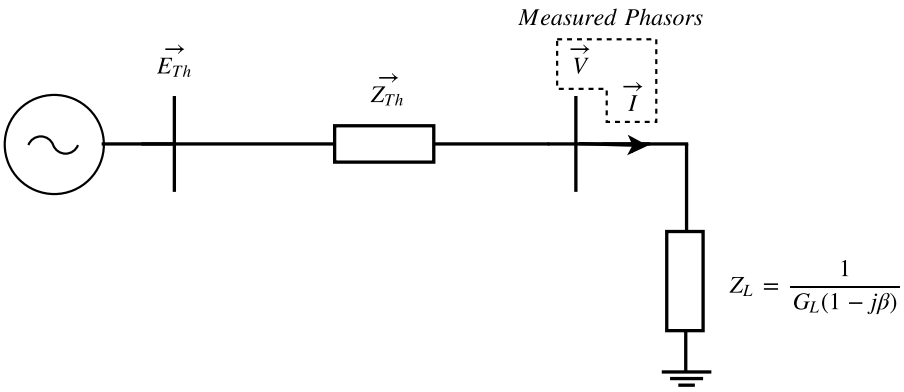


Figure 4.8: A simplified two-bus system.

By using voltage and current phasor measurements taken on a single bus, NLI is calculated straight forward by computing the transmitted active power and the load conductance seen from the bus.

$$NLI = \frac{dP_L}{dG_L} = \frac{P_L^2 - P_L^1}{G_L^2 - G_L^1} \tag{4.31}$$

where

- $P_L^1$ and $G_L^1$ are the active load power and load conductance at the start of change.
- $P_L^2$ and $G_L^2$ are the active load power and load conductance at the end of change.

For a continuous increase in conductance, NLI is positive up to the maximum power transfer limit. NLI becomes zero and indicates that the power limit has been reached, this is equivalent to the nose point on the PV curve and when the load impedance magnitude is equal the Thevenin impedance magnitude.

$$|\vec{Z_{Th}}| = \frac{1}{G_L(1-j\beta)} \tag{4.32}$$

It is important to understand the outcome of equation (4.31). Now consider the load conductance to increase ($dG_L > 0$), and the NLI outcome will be determined by

- $NLI > 0$ A positive change in power, the grid is able to meet the power demand. This is equivalent to the upper part in the PV curve and is an indication of a stable system.

- $NLI < 0$ A negative change in power, the grid is not able to meet the power demand. This is equivalent to the lower part in the PV curve and is an indication of voltage instability.
- $NLI = 0$ No change in power, the grid is not able to meet the demand as the change in conductance is positive. This is equivalent to the nose point on the PV curve.

By considering the circuit in Fig. 4.1, it is possible to compute and plot the trajectories of the NLI with respect to the load conductance. Each curve corresponds to a given magnitude of the Thevenin admittance $Y_{Th}$, as seen in Fig. 4.9 when the load is getting heavier (larger load conductance), the NLI goes towards zero. When the load conductance is equal the Thevenin admittance the maximum power limit is reached and the NLI is equal to zero.

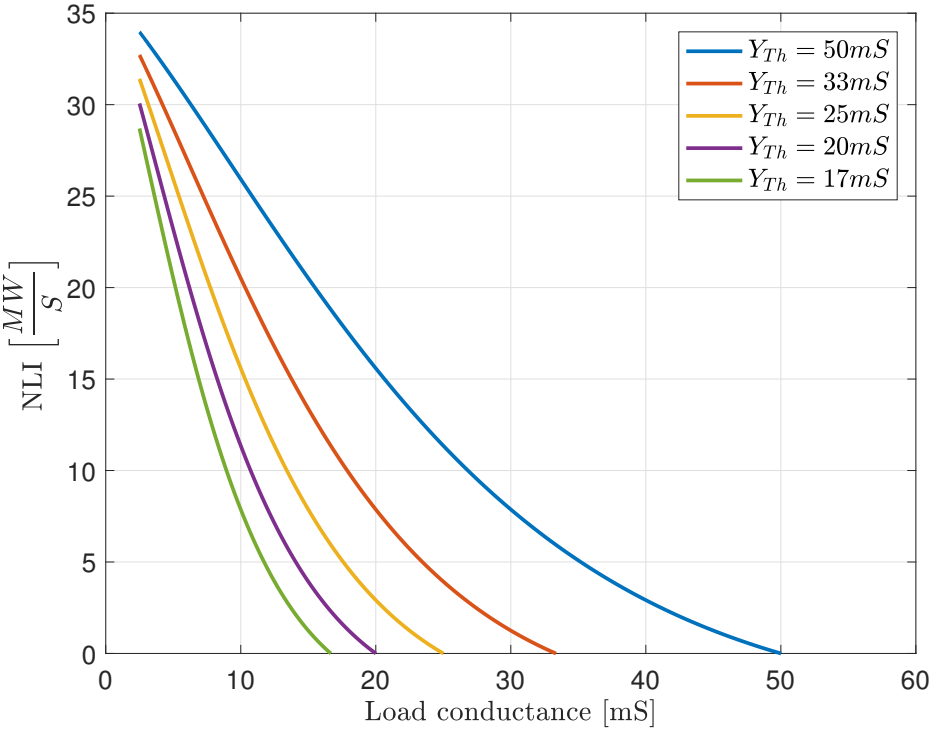


Figure 4.9: Trajectories of the NLI with respect to load conductance.

## 4.7 Signal Filtering

The indicators are constructed based on changes of the load and power. In normal operation, the changes are small, with transients in the grid, noise and error from measurement instruments [10]. In this thesis the measurements are sampled 50 times per second. Therefore, the raw information obtained by the measurement device does not reflect the system response in an illustrative way. By considering only large changes of impedance ($dZ_L$), admittance ($dY_L$) and conductance ($dG_L$) the noise is reduced, and by adding a moving average filter on the indicators, the curves gets smoother and can represent the system response. The moving average filter is expressed by

$$u(i) = \frac{1}{N} \sum_{j=0}^{N-1} x(i-j) \tag{4.33}$$

Where $x$ is the input of a data set, $N$ is the parameter indicating the window size, giving the number of periods of the moving average $u$. Fig. (4.10) illustrates obtained data before and after filtering, the filtered curve is much smoother and truly shows the system response.

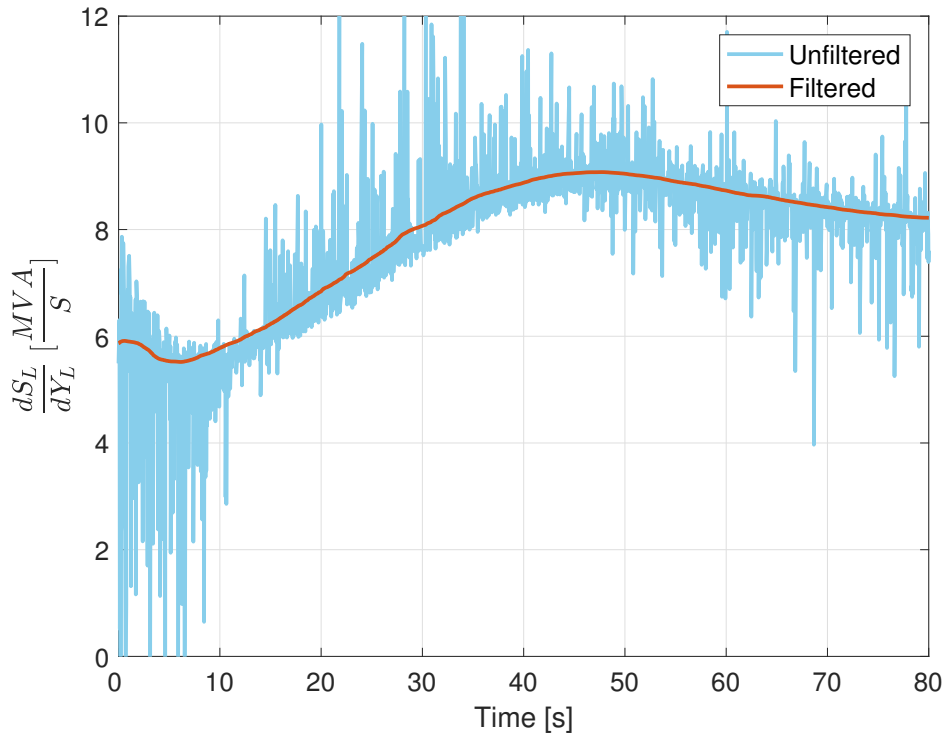


Figure 4.10: S-Y sensitivity before and after filtering.

# Chapter 5

# Power System Setup

This chapter presents the power system to be studied. The laboratory environment and stationary components are introduced for utilization in simulations and experiments.

## 5.1 Laboratory Setup

The system that is studied is installed in the National Smart Grid Laboratory at NTNU/Sintef. Initially, the setup consisted of a 17 kVA generator-set, but the rating of the generator was a bottleneck and not able to cross the loadability limit for this setup, therefore the generator was disconnected, and the setup was connected directly to the main grid. The main grid is also considered more rigid and applicable to real-time conditions and is able to keep the frequency approximately constant.

The setup includes an inductor, a flexible line equivalent, a substation and a variable resistive load. The load is connected to the secondary side of the transformer. The system is presented with the components and its connections in Fig. 5.1. The current flows from the main grid trough the coil, the line equivalent and substation to the load bus supplying power to the variable resistive load.

Depending on the desired scenario, the switches can be modified to be closed or open. In this thesis, the system impedance is chosen to be as large as possible, this is because voltage stability

analysis is the area of study and impedance matching is of interest.

The PMU is connected to the delta coupled side of the transformer, measuring a phase voltage phasor and the corresponding current phasor once each period. The variable inductor, shown in Fig. A.1 is connected to the supply to increase the system impedance. The coil is set to 1 mH, giving the impedance of the coil to be

$$X_{Inductor} = j\omega L = j2\pi \cdot 50 \cdot 1mH = j0.31\Omega \tag{5.1}$$

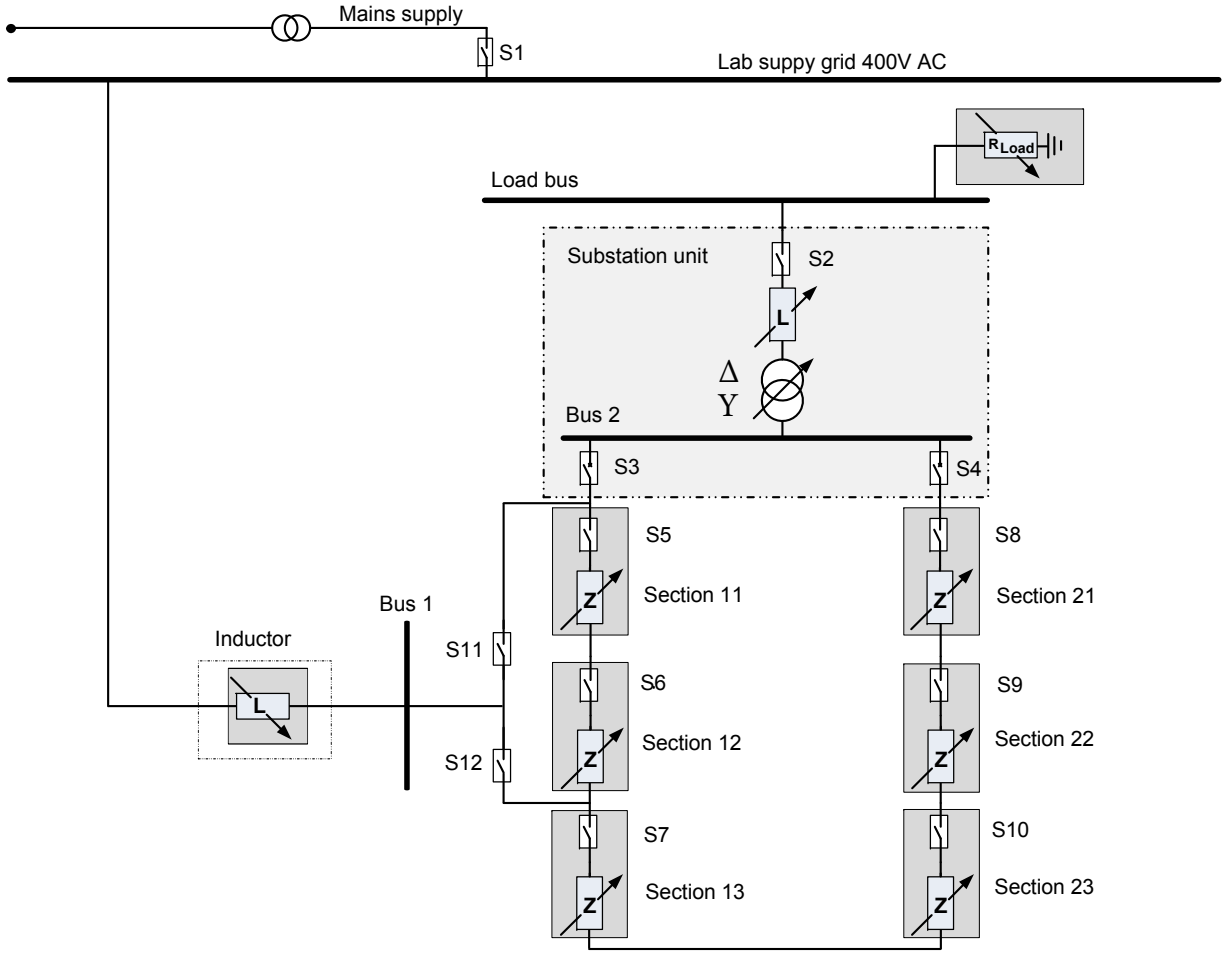


Figure 5.1: Laboratory setup utilized in experiments.

### 5.1.1 Flexible Line Equivalent

Most of the electrical energy is transported from the transmission, or sub transmission, network to distribution networks in order to bring it to the consumer [1]. Concerning voltage stability studies, it is interesting to monitor a distribution network that can operate close to the loadability limit and even beyond the limit. In this model, shown in Fig. A.2, the line equivalent is built of several reactors and resistances in series. The number of windings in the reactors modifies its inductance. The three possible settings are 0.62mH, 1.24mH and 2.48mH. At 50 Hz frequency, the reactance is

$$jX_{Line} = j\omega L = j2\pi \cdot 50 \cdot \begin{bmatrix} 0.62 \\ 1.24 \\ 2.48 \end{bmatrix} mH = j \begin{bmatrix} 0.19 \\ 0.39 \\ 0.78 \end{bmatrix} \Omega \tag{5.2}$$

It is possible to bypass the resistances using switches, each section has four resistances with separate switches. Fig. 5.2 presents how each section is connected.

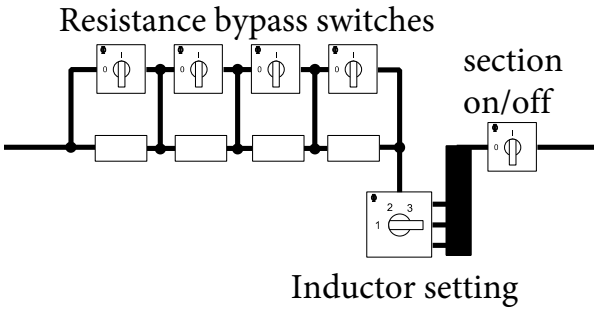


Figure 5.2: Connections of a section in the line equivalent model.

Considering Fig. 5.1, switch S11 is open and S12 is closed, the current can flow in two paths, one path is through section 11 and 12, the other is through section 13, 21, 22 and 23. Operating with the inductors switch at the largest inductance setting and all the resistance bypass switches open, from Appendix A, Section A.2 the impedances of branch 1, consisting of section 13, 21, 22 and 23 are calculated to be

$$Z_{Line\,1} = Z_{section\,13} + Z_{section\,21} + Z_{section\,22} + Z_{section\,23} = 2.78 + 4 \cdot j0.78 = 2.78 + j3.12\Omega \quad (5.3)$$

The impedance of the other branch consisting of two sections, section 11 and 12 is

$$Z_{Line\,2} = Z_{section\,11} + Z_{section\,12} = 0.67 + 2 \cdot j0.78 = 0.67 + j1.56\Omega \quad (5.4)$$

### 5.1.2 Substation

A substation can be considered as a point of electrical connection where the transmission lines, transformers, generating units, system monitoring and control equipment are connected together [1]. Therefore, it is at substations that the flow of electrical power is controlled, voltages are transformed from one level to another and system security is specified by automatic protective devices.

The substation unit is shown in Fig. A.3, this laboratory model consists of:

- 400 V/400 V, Y-Δ, 25 kVA transformer
- A bus combining the two feeders of the flexible line equivalent
- Another line equivalent representing the line impedance to the substation.

The relative short circuit voltages in the transformer are assumed to be approximately $e_z = 2.6$ and $e_r = 2$. [17] The relative reactive short circuit voltage is

$$e_x = \sqrt{e_z^2 - e_r^2} = \sqrt{2.6^2 - 2.0^2} = 1.7 \quad (5.5)$$

Calculating the short circuit resistance and reactance

$$R_{Transformer} = \frac{e_r}{100} \cdot \frac{V_N^2}{S_N} = \frac{2}{100} \cdot \frac{400V^2}{25kVA} = 0.13\Omega \quad (5.6)$$

$$X_{Transformer} = \frac{e_x}{100} \cdot \frac{V_N^2}{S_N} = \frac{1.7}{100} \cdot \frac{400V^2}{25kVA} = j0.11\Omega \quad (5.7)$$

The transformer impedance is then

$$Z_{Transformer} = R_{Transformer} + X_{Transformer} = 0.13 + j0.11\Omega \tag{5.8}$$

Line equivalent representing the line impedance to the substation can be chosen to be different inductances, to be either 0.4, 0.8 or 1.6 mH. So the possible outcomes of the substation reactance at 50 Hz frequency is

$$X_{Substation} = j\omega L = j2\pi \cdot 50 \cdot \begin{bmatrix} 0.4 \\ 0.8 \\ 1.6 \end{bmatrix} mH = j \begin{bmatrix} 0.12 \\ 0.25 \\ 0.50 \end{bmatrix} \Omega \tag{5.9}$$

As mentioned in Section 5.1, the system impedance is preferred to be as large as possible.

$$Z_{Substation} = Z_{Transformer} + X_{Substation} = 0.13 + j0.11 + j0.50 = 0.13 + j0.61\Omega \tag{5.10}$$

### 5.1.3 Load

The load in the laboratory setup consists of heating elements that are purely resistive, and are a constant impedance load. The resistance is set by the load controller shown in Fig. A.4, and the heating elements are inside a water cooled cabinet shown in Fig. A.5. By adjusting the resistances, the load impedance is increased/decreased. Available settings are listed in Table A.1.

As mentioned in Section 3.2, the power of a constant impedance load is voltage dependent. The load is connected to the load bus and the component is shown as $R_{Load}$ in Fig. 5.1.

## 5.2 Simplifications and Base Values

A per phase equivalent circuit is representing the power system in Fig. 5.3. The stiff main supply is represented as a voltage source supplying the circuit with power through the simplified

components to the receiving end where the load impedance connected. The PMU located at the load-bus measuring the phasors of voltage and current.

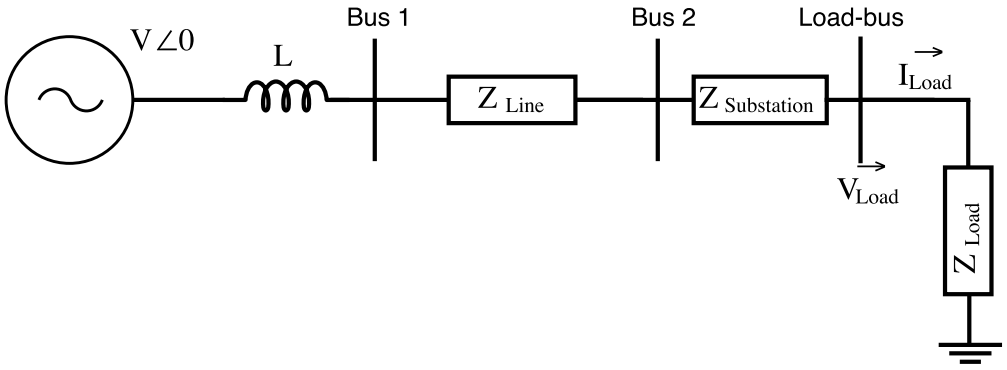


Figure 5.3: Simplified per phase equivalent for the laboratory power system.

The per unit system is utilized in computing of the indicators, this is needed to have a reasonable and comparable scale. The line-to-line voltage is 400 V, therefore the reference voltage magnitude is set to 400 V. The reference apparent power is set to 25 kVA, the same as the nominal power of the transformer. The base values are calculated in (5.11) and (5.12).

$$I_{Base} = \frac{S_{Base}}{\sqrt{3}V_{base}} = \frac{25kVA}{\sqrt{3}\cdot 400V} = 36.1A \tag{5.11}$$

$$Z_{Base} = \frac{V_{Base}}{\sqrt{3}I_{Base}} = \frac{400V}{\sqrt{3}\cdot 36.1A} = 6.4\Omega \tag{5.12}$$

Table 5.1: Base values for the laboratory power system.

| **Type** | **Value** |
|---|---|
| Apparent power base, $S_{base}$ | 25 kVA |
| Voltage base, $V_{Base}$ | 400 V |
| Current base, $I_{Base}$ | 36.1 A |
| Impedance base, $Z_{Base}$ | 6.4 Ω |

# Chapter 6

# Case Study and Results

This chapter presents descriptions of two cases with results and discussions to verify the implementation of the indicators and the methods of estimating the Thevenin impedance and the corresponding maximum power transfer limit.

The first case consists of load increase of a weakened network where the system impedance is larger than the smallest possible load impedance. The second case involves a line contingency when the current is relatively high, the disturbance causes the system impedance to change radically. These two scenarios were designed to emulate the extremes of two conditions that may occur in a real distribution network.

MATLAB simulation is done because it is important to be aware of the theoretical behavior of the system before doing the laboratory tests. In addition, the system was modeled considering the laboratory setup described in Section 5.1 to study the behavior of the voltage stability indicators and the two methods of estimating the Thevenin impedance under ideal conditions and illustrate the ideal computations. There were times where the load impedance magnitude was constant in the MATLAB simulation, meaning there is no change in load ($dZ_L$, $dY_L$ and $dG_L$), meaning the denominator of the indicators would be equal zero. Therefore, there was a need for a very small variation in the MATLAB simulations were the load impedance magnitude was constant. The small variation is not visible or has any effect on the performance on the indicators.

Measurements are taken at the load bus, involving phasors of voltage and current and are the only measurements used in the computation. The measurements are done in a single phase, thus assuming a symmetrical system. The reporting frequency of the PMU is 50Hz, meaning there are 50 measurements of voltage and current phasors every second. The measurements are stored and processed with the theory algorithms and filters, this is not an option for real-time tools as the data has to be computed momentarily.

All the indicators are plotted in per unit values. It is noted that the limit for all indicators are zero, so the unit is not important as the trajectories are the same for all scales.

In addition to the results in this thesis, there are made animations in MATLAB based on the laboratory experiments [18]. This emphasizes how well the indicators reveal the distance to voltage instability. The animations capture both laboratory experiments in various plots, it is possible to see the indicators trajectories with the corresponding PV curves as operation points moving with time.

To have an idea of the Thevenin impedance magnitude, $Z_{Th}$, parameters from the laboratory components are utilized to calculate a system impedance $Z_{Sys}$. With this in mind, it is possible to establish the maximum power transfer limit and compare the estimated Thevenin impedance to the actual system impedance.

## 6.1 Case Study on Increased Load Demand

To test the reliability of the indicators it is of interest to reach the maximum loadability for the system. To achieve this, the system impedance has to be larger than the load impedance as described in Section 4.1. Now consider Fig. 6.1 and the switch states that are listed in Table 6.1. All the sections in the flexible line equivalent are connected in series with the inductor and the substation. The system impedance is now as large as possible, this is necessary to have the desired scenario.

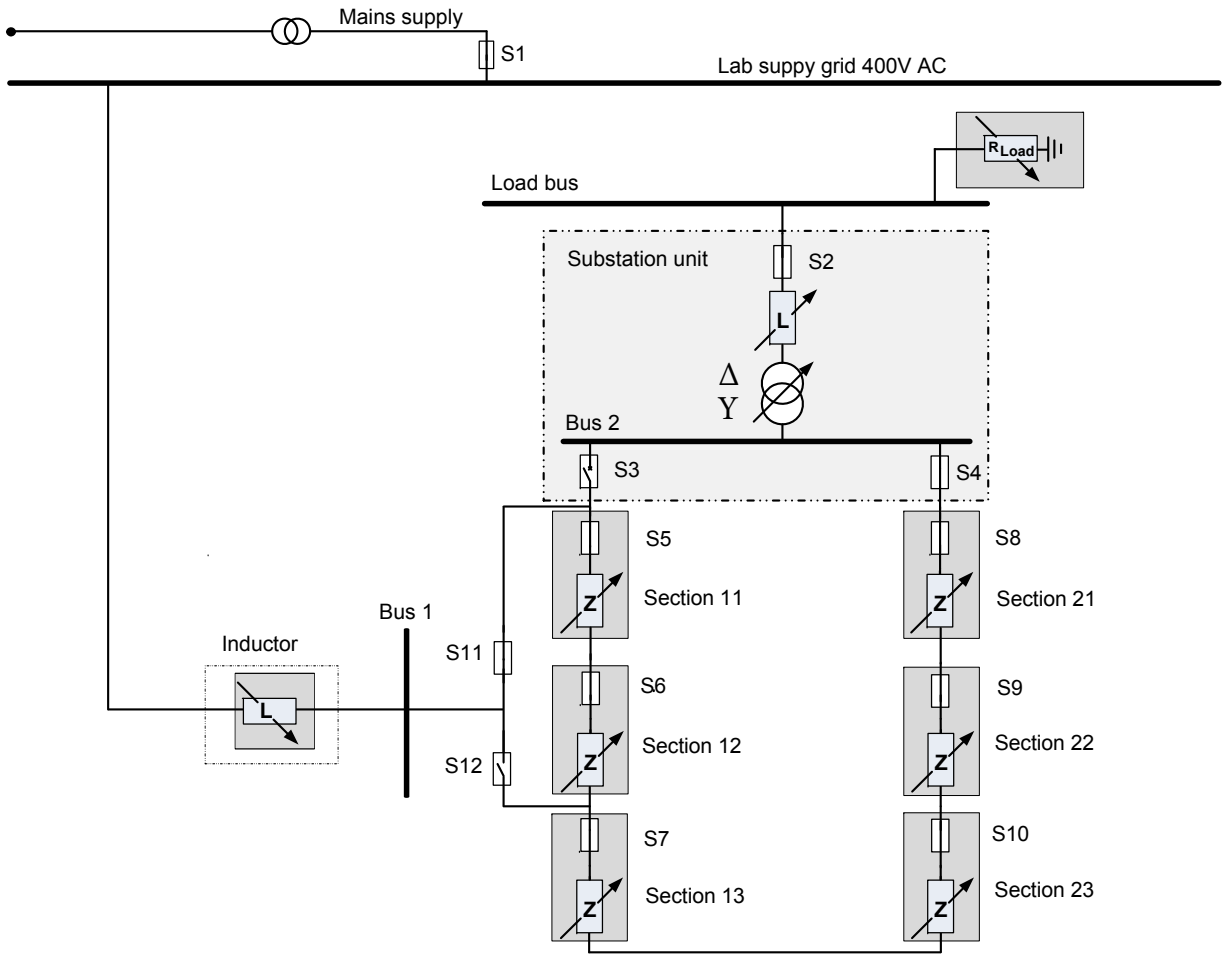


Figure 6.1: The laboratory setup configured to largest possible system impedance.

Table 6.1: Switch connections and initial states

| **Switch** | **Connection** | **Initial state** |
|---|---|---|
| S1 | Main supply | Closed |
| S2 | Transformer to load bus | Closed |
| S3 | Feeder from line equivalent to substation | Open |
| S4 | Feeder from line equivalent to substation | Closed |
| S5, S6, S7, S8, S9 & S10 | Distribution network sections | Closed |
| S11 | Connection point on the line equivalent | Closed |
| S12 | Connection point on the line equivalent | Open |

The system impedance $Z_{Sys}$ can be calculated based on the components parameters. The short circuit impedance at the main supply is neglected because it is assumed to be very small. The system impedance is

$$Z_{Sys} = X_{Inductor} + Z_{Line\,1} + Z_{Line\,2} + Z_{Substation} \tag{6.1}$$

$$Z_{Sys} = j0.31 + 2.78 + j3.12 + 0.67 + j1.56 + 0.13 + j0.61 = 3.58 + j5.60\Omega \tag{6.2}$$

$$|Z_{Sys}| = \sqrt{3.58^2 + 5.60^2} = 6.65\Omega \tag{6.3}$$

In this case study, the system impedance is expected to remain constant due to connection to the main grid with a constant frequency. The resistances could eventually increase due to heating but it is not taken into consideration. In the S-Z and S-Y method, the $X/R$ ratio of the Thevenin impedance must be set in advance. In this setup the ratio in $Z_{Sys}$ is approximately 1.6. From Table. A.1 the minimum load impedance, $Z_{Load}$ is estimated to be 5.6Ω which obviously is less than the calculated system impedance $Z_{Sys}$. The load is manually controlled by switches described in Section 5.1.3, initially the load impedance is infinite, thus no current flowing. The load impedance is gradually decreased to 7.8Ω over the first 600 s, then varying the load impedance between 7.8Ω and 7.4Ω from $t$ = 600 s to $t$ = 1000 s. After 1000 s. the load impedance is decreased gradually to the minimum value of 5.6Ω, at this time the load impedance is expected to be larger than the system impedance. The events are listed based on time in Table 6.2.

Table 6.2: Increased load demand events.

| **Load impedance event** | **Time [s]** |
|---|---|
| Connected to the power system and gradually decreased to 7.8Ω | 0-600 |
| Varying between 7.8Ω and 7.4Ω | 600-1000 |
| Gradually decreased from 7.4Ω to 5.6Ω | 1000-1250 |
| At its minimum value, meaning maximum power | 1250- |

### 6.1.1 MATLAB Simulation

Before doing laboratory tests it is important to know the theoretical behavior when the system is exposed to events. A simplified single-phase diagram of the power system is shown in Fig. 6.2. The main supply from the laboratory is represented as a voltage source with the reference angle $V\angle 0$, the inductor reactance $X_{Inductor}$, the flexible line equivalent $Z_{Line1}$ and $Z_{Line2}$, and the substation unit $Z_{Substation}$.

MATLAB simulation utilizes voltage and current phasors calculated in (6.6) and (6.7) to compute the indicators and the Thevenin impedance seen from the load bus. As seen in Fig. 6.3, the load impedance is modeled as the scenario described in Section 6.1. The system impedance is modeled as a constant impedance based on the system components parameters. At $t$ = 1090 s, the load impedance magnitude is equal to the system impedance magnitude.

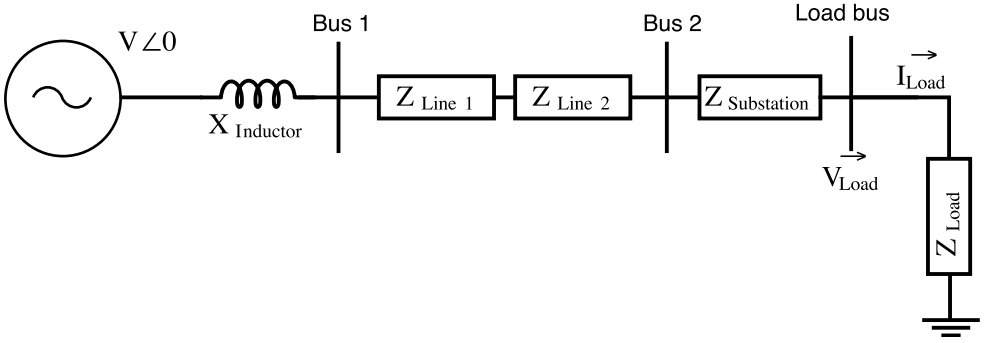


Figure 6.2: Simplified mode of the power system studied.

$$V = \frac{400}{\sqrt{3}} \angle 0 \tag{6.4}$$

$$Z_{Sys} = X_{Inductor} + Z_{Line\,1} + Z_{Line\,2} + Z_{Substation} \tag{6.5}$$

$$I_{Load} = \frac{V}{Z_{Sys} + Z_{Load}} \tag{6.6}$$

$$V_{Load} = V - I_{Load} Z_{Sys} \tag{6.7}$$

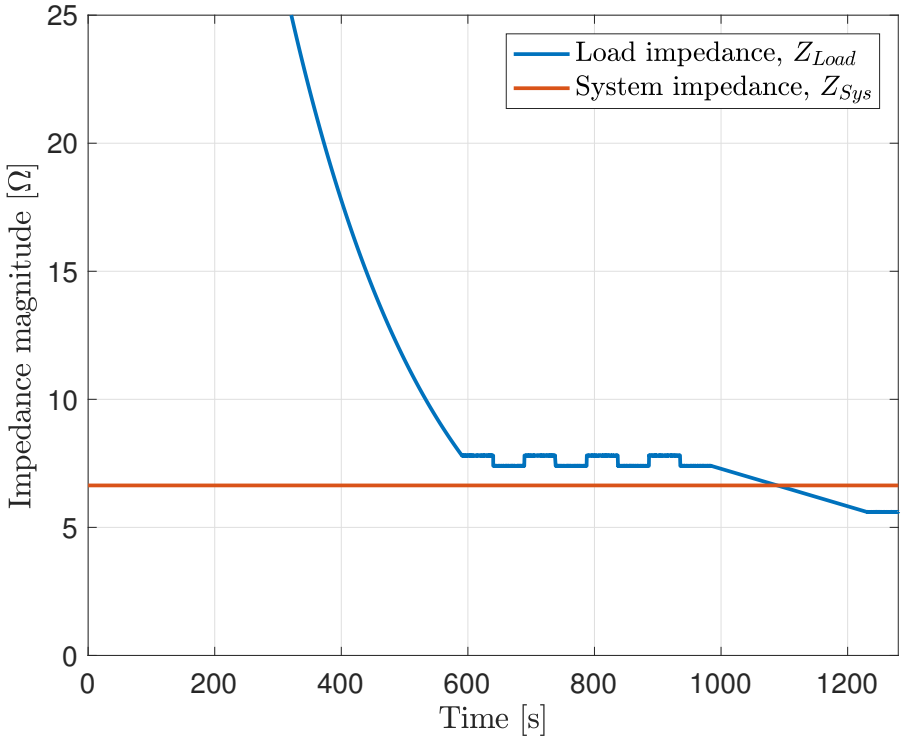


Figure 6.3: Load and system impedance versus time.

As seen in Fig. 6.4a the load power is able to increase as the load impedance decrease until the maximum power transfer limit is reached at $t$ = 1090 s. After this time, the power decreases as the load impedance decreases. The PV curve in Fig. 6.4b shows the power-voltage characteristic at the load bus during the simulation period. The figure shows that the voltage gradually drops when the power increases until the nose point, maximum power is then 7.83 kW at 228 volts. The voltage *and* the power decreases after the maximum loadability limit is reached, the voltage minimum value is 208 volts when the load power is 7.76 kW.

Fig. 6.5 shows the indicators during load events. It can be seen that when the load is light (load impedance is high), the S-ZI is negative while S-YI and NLI are positive. The NLI and S-YI trajectory are equal as the load is purely resistive, meaning the admittance contains only conductance and apparent power only contains active power. As the power starts to increase the indicators show their trajectories as expected. As the load impedance is equal to the system impedance, at $t$ = 1090 s, all indicators are equal to zero, this is corresponding to the nose point of the PV curve and is the maximum power transfer limit. The indicators change sign when the load impedance is further decreased and indicates voltage instability.

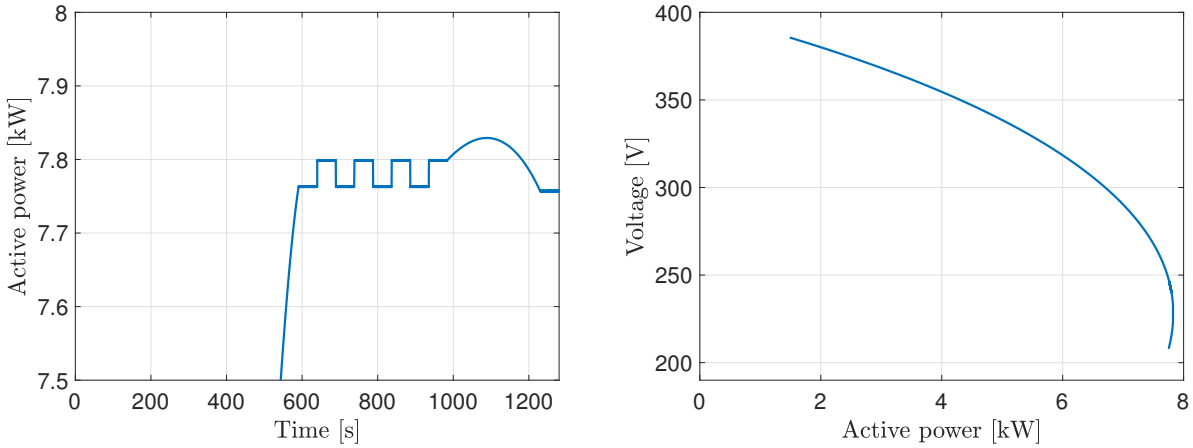


(a) Load power versus time.

(b) PV characteristic.

Figure 6.4: Power and PV characteristic of the load increase events.

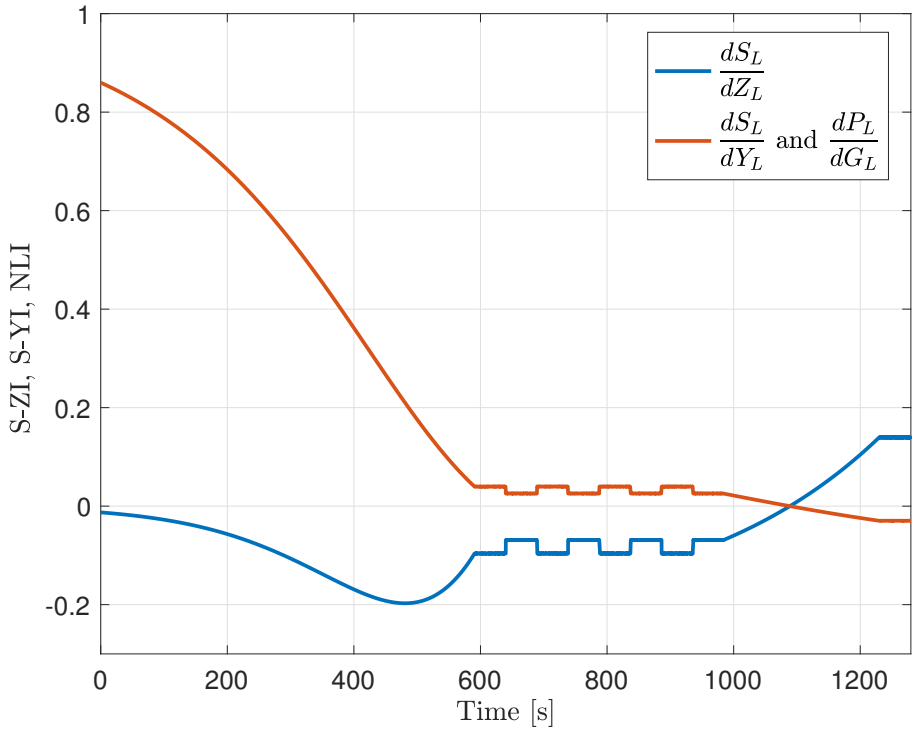


Figure 6.5: Indicators versus time, the indicators show pattern compared to loading.

Fig. 6.6a show a trajectory of the S-ZI versus load impedance magnitude during the load increase period. The trajectory recognizable from Section 4.3, as the load impedance is large the indicator is negative and the system is within the voltage stability limit. As the load power increases (load impedance decrease), the indicator decreases before it changes direction and goes

towards zero. The indicator crosses zero at the point where the load impedance is equal to the system impedance as predicted.

Fig. 6.6b depicts the S-YI and NLI as a function of the load conductance and admittance magnitude. Since the load impedance is purely resistive the trajectories are completely the same for both indicators. The apparent power consists of active power and the admittance contains only conductance. As the admittance increases, the impedance decreases and the zero crossing corresponds with the impedance matching. If the conductance is increased further, the indicator becomes negative and indicates voltage instability.

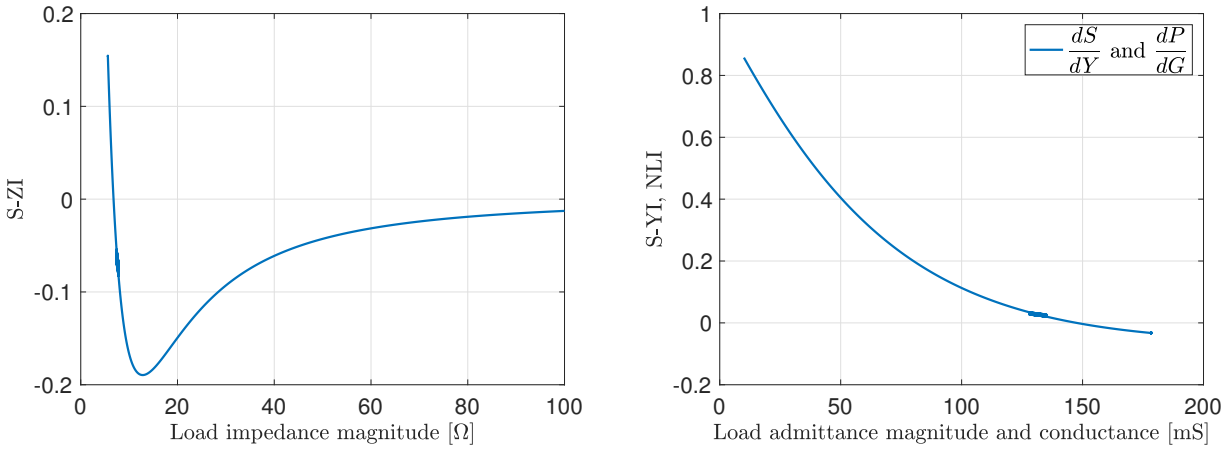


(a) S-ZI versus load impedance magnitude.

(b) S-YI and NLI as a function of load admittance magnitude and conductance.

Figure 6.6: The indicators versus their respective unit.

The Thevenin impedance computed from S-Z method and S-Y method are in this MATLAB simulation equal to each other. Fig. 6.7 shows the load impedance and the Thevenin impedance magnitudes obtained from S-Z and S-Y method described in Section 4.3.2 and Section 4.4.2. As can be seen, the Thevenin impedance is approximately equal the system impedance, which gives a good indication of the reliability of the methods for estimating the Thevenin impedance for this simulation.

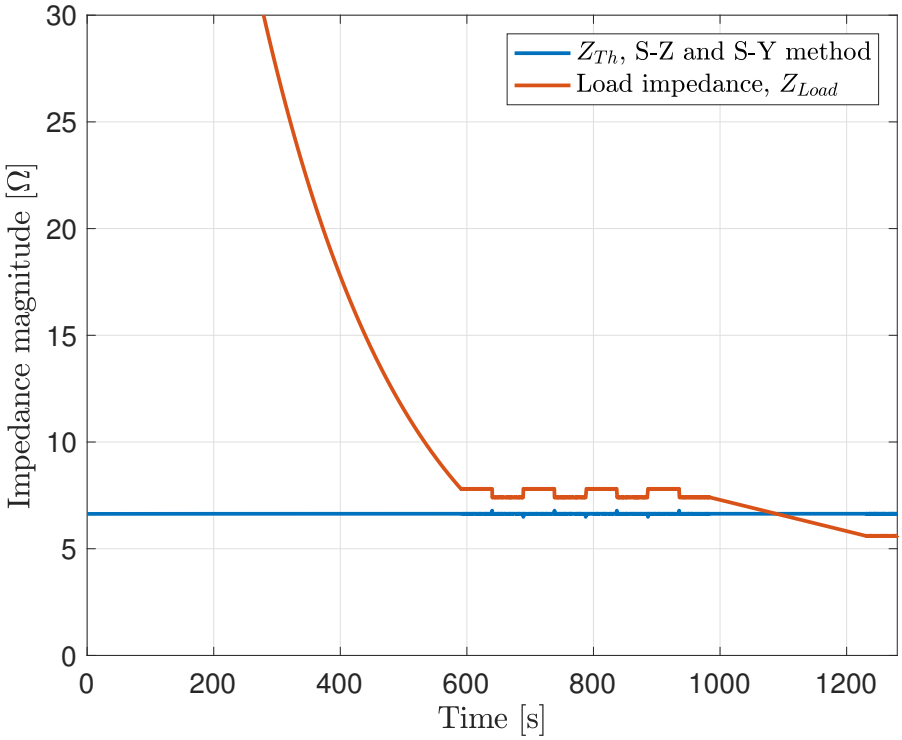


Figure 6.7: Thevenin impedance seen from the load bus.

### 6.1.2 Laboratory Experiment

A laboratory test is done utilizing the setup described in Section 6.1, by regulating the variable load resistance, described in Section 5.1.3, the load demand adjusts accordingly.

During this scenario, it is interesting to see how the indicators respond to the small disturbances exposed to the system, and when the indicators reveal that the maximum loadability limit is reached. Fig. 6.8a shows the measurements of voltage and current magnitudes during the scenario of load demand change. As can be seen, the voltage decreases and the current increases as the load demand is higher. The increase in current makes the voltage drop across the system impedance to become larger, giving a smaller voltage at the load bus. Active load power is illustrated in Fig. 6.8b, the figure shows that the maximum power is at $t = 1110$ s, and from $t = 1110 - 1280$ s the power gradually decreases as a result of the maximum power transfer limit breach.

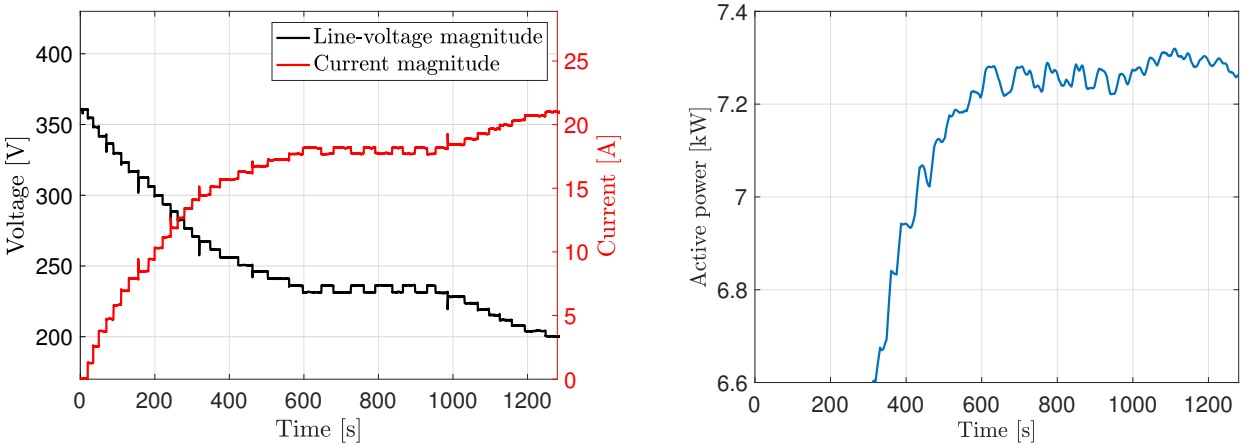


(a) Voltage and current magnitudes versus time.

(b) Active power versus time.

Figure 6.8: Measurements done during the experiment with an increase of load demand.

The power-voltage characteristic is displayed in Fig. 6.9, the power is increased while voltage is dropping, then at the nose point of the PV curve, the load impedance is equal to the system impedance. When a further decrease of the load impedance, the power *and* the voltage decreases as described in Section 3.1.

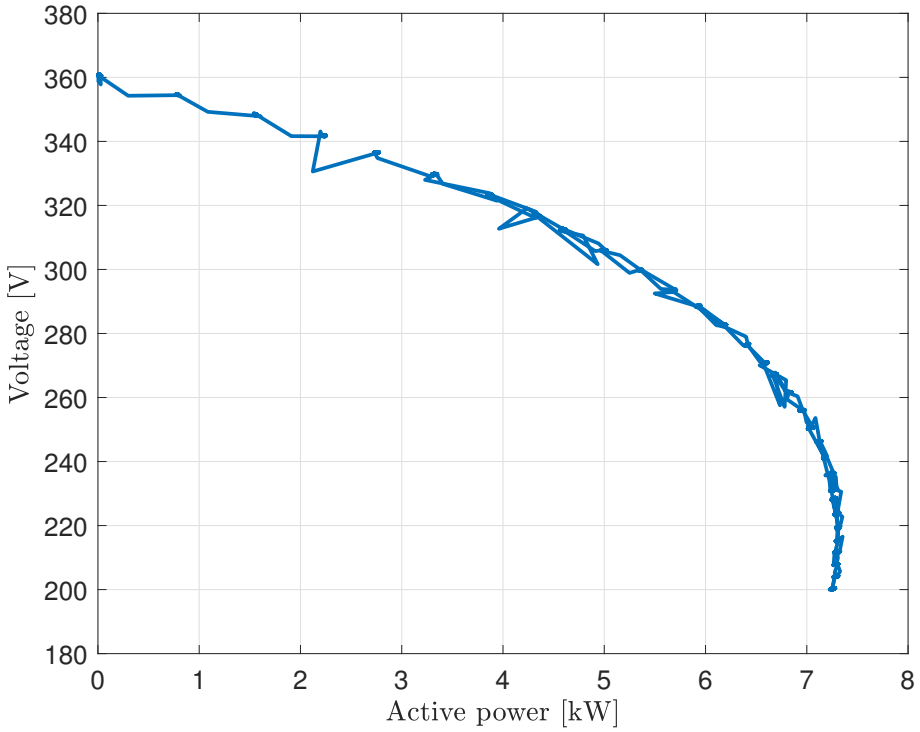


Figure 6.9: Power-voltage characteristic of the load.

Fig. 6.10 illustrates the three indicators during the experiment, as can be seen when the load is within the voltage stability limit, the S-YI and NLI indicators are positive while S-ZI is negative. As expected the NLI trajectory follows S-YI as the load is purely resistive, meaning the admittance contains only conductance. Zero crossing of the indicators are at following times

- $S-ZI=0$ at $t=1117s$
- $S-YI=0$ at $t=1125s$
- $NLI=0$ at $t=1110s$

The peak load power is detected at $t=1110$ s. For this experiment the S-ZI and S-YI detect the maximum power transfer condition some seconds after than actual maximum power transfer limit, the deviation is obviously acceptable. NLI zero crossing is very precise compared to maximum power transfer limit.

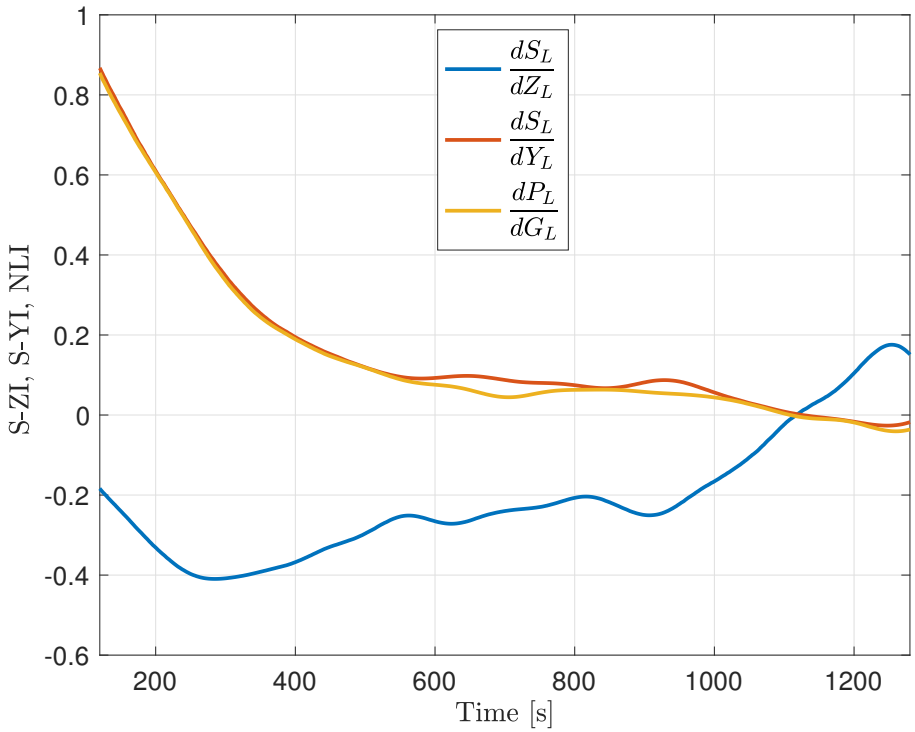


Figure 6.10: S-ZI, S-YI and NLI versus time.

Fig. 6.11 shows the trajectory of the S-ZI with respect to load impedance magnitude. As expected the S-Z sensitivity indicator shows the same pattern at the theoretical trajectory described in Section 4.3.2 and shown in Fig. 4.4. When the load impedance is high, the S-ZI is negative, as the load impedance decreases the indicator goes down before reversing its path. The indicator starts rising when decreasing the load impedance even more and is equal to zero when the load impedance is equal to 6.31Ω. At this point, the load impedance is equal to the estimated Thevenin impedance.

S-YI with respect to load admittance magnitude together with NLI versus load conductance is plotted in Fig. 6.12. As expected the S-Y sensitivity indicator shows the same predicted pattern as the theoretical trajectory described in Section 4.4.2 and shown in Fig. 4.6. When the load power increases the load admittance increases. The zero crossing occurs when the admittance is 0.158 S. meaning the load impedance is 6.33 Ω. This corresponds to the nose point on the PV curve. The NLI has the same pattern as described in Section 4.6, and since the load is completely resistive, the conductance is equal the admittance. With this condition, the two indicators follow each other and cross zero at the same value.

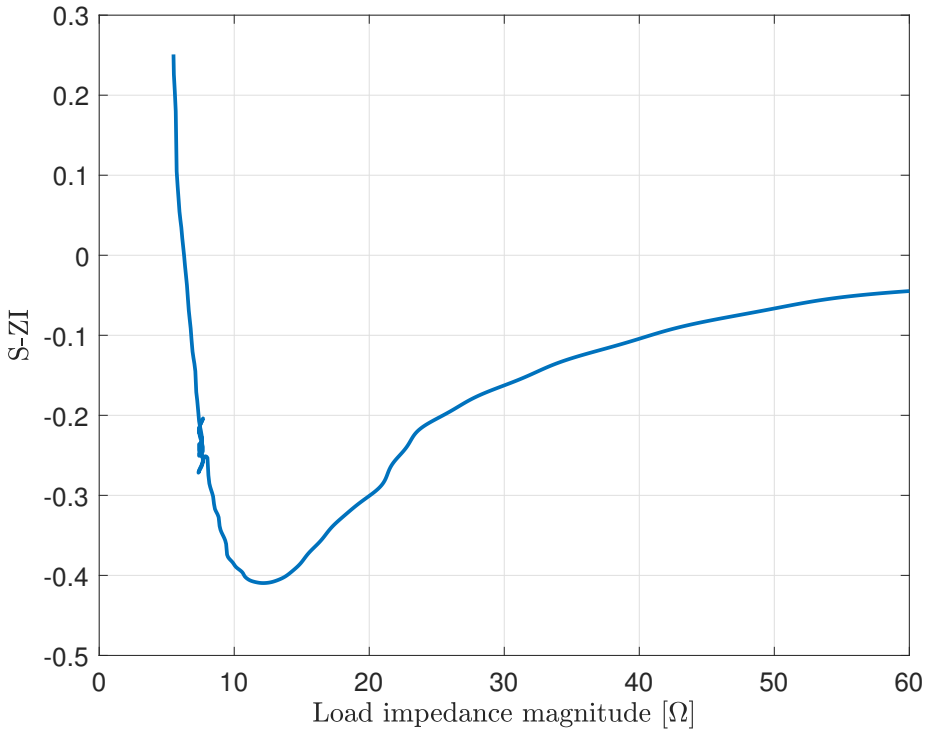


Figure 6.11: S-ZI versus load impedance magnitude.

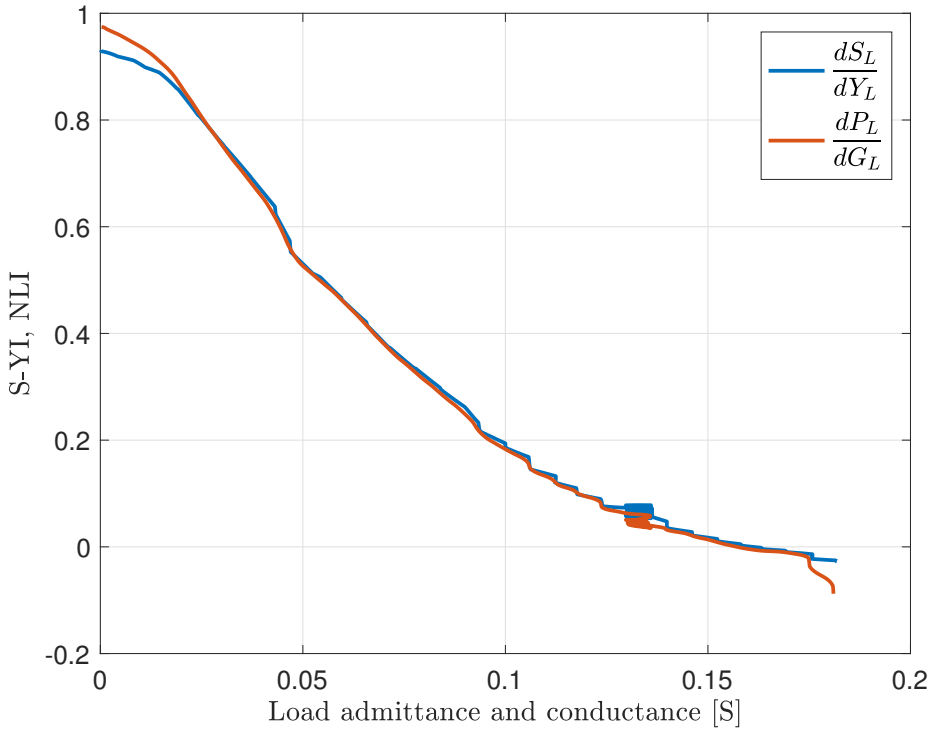


Figure 6.12: Comparable patterns from S-YI and NLI.

Fig. 6.13 shows the load impedance ($Z_{Load}$) and the Thevenin impedances ($Z_{Th}$) estimated from the S-Z method and the S-Y method. As the figure shows the two methods generate comparable impedances during this experiment. The estimated Thevenin impedances are close to predicted system impedance described in Section 6.1, as the system impedance magnitude was calculated beforehand to be 6.78Ω. The magnitudes of Thevenin impedance and load impedance are equal at 6.31Ω, at approximately $t$ = 1125 s, which is slightly after the maximum power transfer limit. There are large variations of the estimated Thevenin impedance when the load is light. From (4.3), it is possible to compute estimated maximum power based on the Thevenin impedance and phasors of current and voltage. The estimated maximum power and actual load power is shown in Fig. 6.14. As seen in the graph, the power margin is clearly illustrated when the estimated maximum loadability and load power are plotted together. At the start of the scenario the estimation of power margin has large variation. The estimated power margin after $t$ = 500 s is varying between 0.2 kW and 0.4 kW on both approaches. Ideally the maximum loadability limit should be equal the load power at the border to voltage instability. However, the estimated maximum power is above the actual load power at all times in this computation.

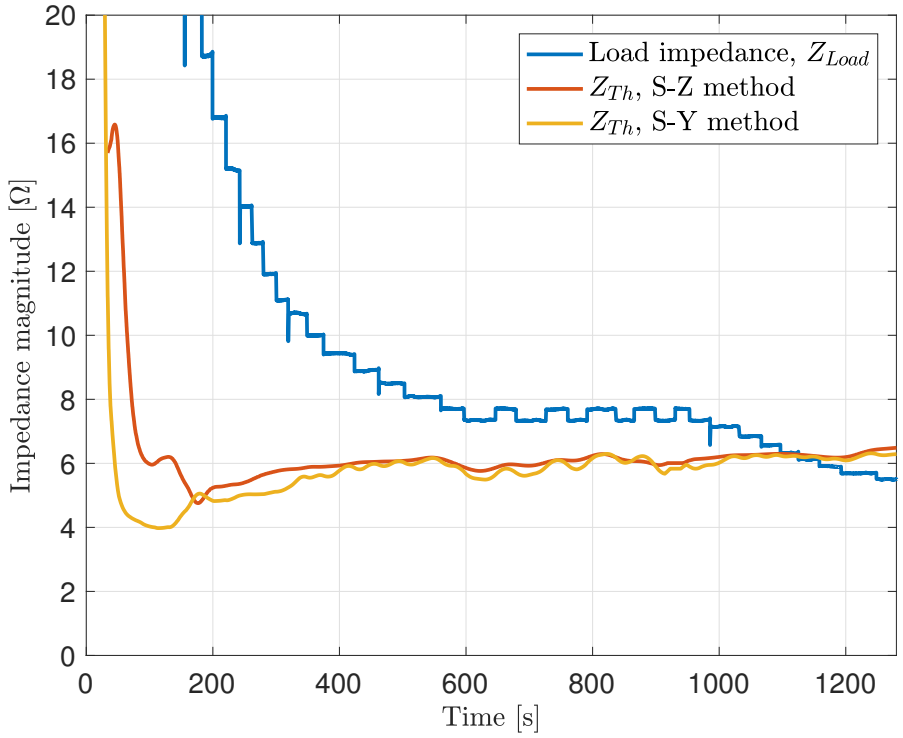


Figure 6.13: The load impedance and two estimated Thevenin impedances versus time.

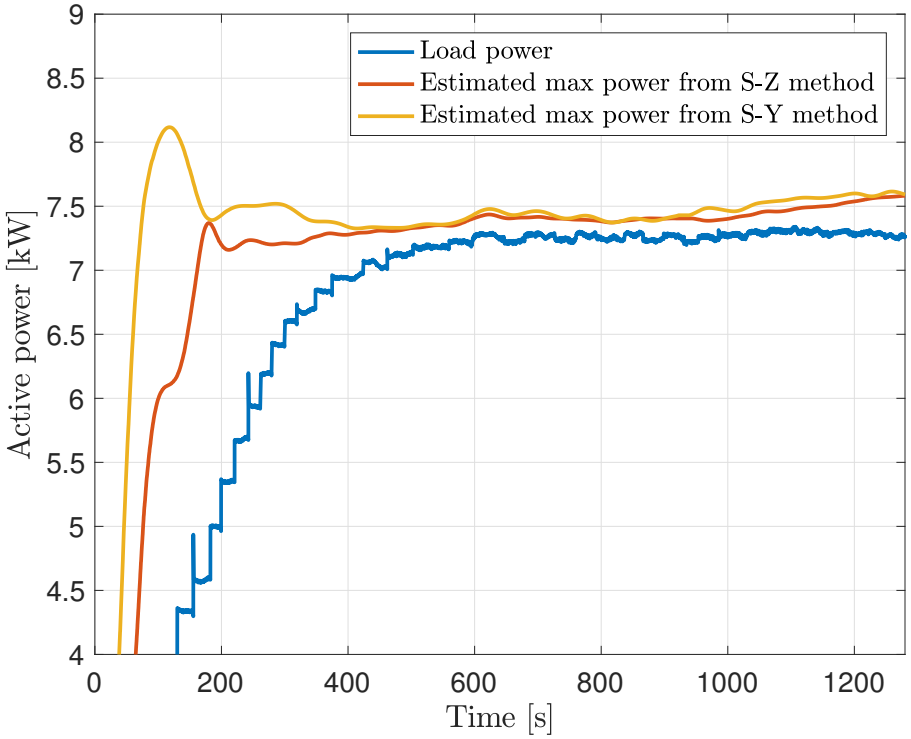


Figure 6.14: Actual load power and two estimated maximum power versus time.

As described in section 4.5, the ratio of $X_{Th}/R_{Th}$ must be set before the estimation of the Thevenin impedance can be done. In this experiment the ratio was set to 1.6, that is equal the $X/R$ ratio of $Z_{Sys}$. In normal operation the Fig. 6.11 is unavailable unless an occurrence of the maximum power transfer condition is fulfilled. To handle this, it is possible to have an estimate of the curve by using the Thevenin impedance to draw the trajectory and compare with the S-ZI obtained from measurements. By using (4.12), a trajectory in Fig. 6.15a is drawn. The S-ZI illustrated by a red dot is directly calculated from phasor measurements at $t = 600$ s where the load impedance is equal 7.8 Ω. As the red dot is almost correct, the estimation of the Thevenin impedance is accurate.

The same procedure is done to draw the trajectory of S-YI illustrated in Fig. 6.15b, based on (4.22) the S-YI is computed by using the Thevenin impedance and voltage and current phasors. The load admittance is 128 mS at $t = 600$ s as the red dot indicating the operation point. At zero crossing of the S-ZI and S-YI, the Thevenin impedance is equal to the load impedance.

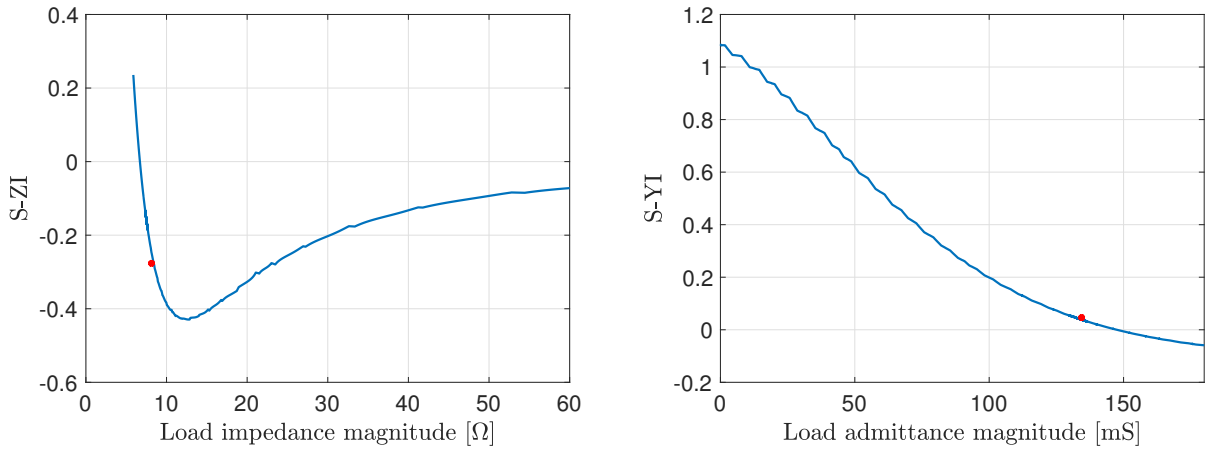


(a) S-ZI versus load impedance magnitude.

(b) S-YI versus load admittance magnitude.

Figure 6.15: Sensitivity indicators computed based on the Thevenin impedance.

### 6.1.3 Discussion

Local PMU measurements are utilized to compute the different indicators and two methods estimate the Thevenin impedance, in addition to the estimated maximum power. It is convincingly validated that the indicators successfully detect the maximum power transfer limit and continue to give "worse" values as the maximum transfer level is passed, which is the expected response of a good indicator. Hence the indicators show overall good performances with the ability to detect voltage instability. The laboratory experiment patterns of the indicators were expected in the theory described in Chapter 4 and comparable to the ideal computations by MATLAB simulation.

The Thevenin impedance was estimated of the S-Z and S-Y method. Accuracy was good compared to the expected value of the laboratory components impedance $Z_{Sys}$. The exceptions were then the load power was low in the laboratory experiment. The reason is that there is a small difference among the S-ZI and S-YI trajectories when there is low power transfer. The maximum power estimation is strongly influenced by the Thevenin impedance and has large variations when load is light, this disadvantage is unimportant because the operating point is far from the voltage stability limit.

The estimated maximum power did not detect exceedance of the maximum power transfer limit and showed a positive power margin which was not the case. It cannot be concluded that the ultimate power limit is the estimated maximum power.

It is essential to remember that the Thevenin impedance is a measure of the temporary strength of the power system, and should not be used as the final constraint of the network. The system discovers its ultimate capacity only when the nose point on the PV curve is reached which corresponds to the indicators zero crossing.

## 6.2 Case Study on Line Contingency

As mentioned in Section 3.3, one of the most common situations for voltage stability issues is when the network is being weakened by a large disturbance. By utilizing the setup in Fig. 6.16 it is possible to replicate a line trip on one of the parallel lines transporting power to the load.

In order to study how the power system operation conditions changes during a large disturbance, a line contingency is forced by simply opening switch S3 as seen in Fig. 6.16. Initially, the current is flowing through both switch S3 and switch S4. At $t = t_1$ switch S3 is opened, making all power to flow through switch S4. This event increases the system impedance drastically and has a large effect on the voltage and current magnitudes. The initial switch states are listed in table 6.3.

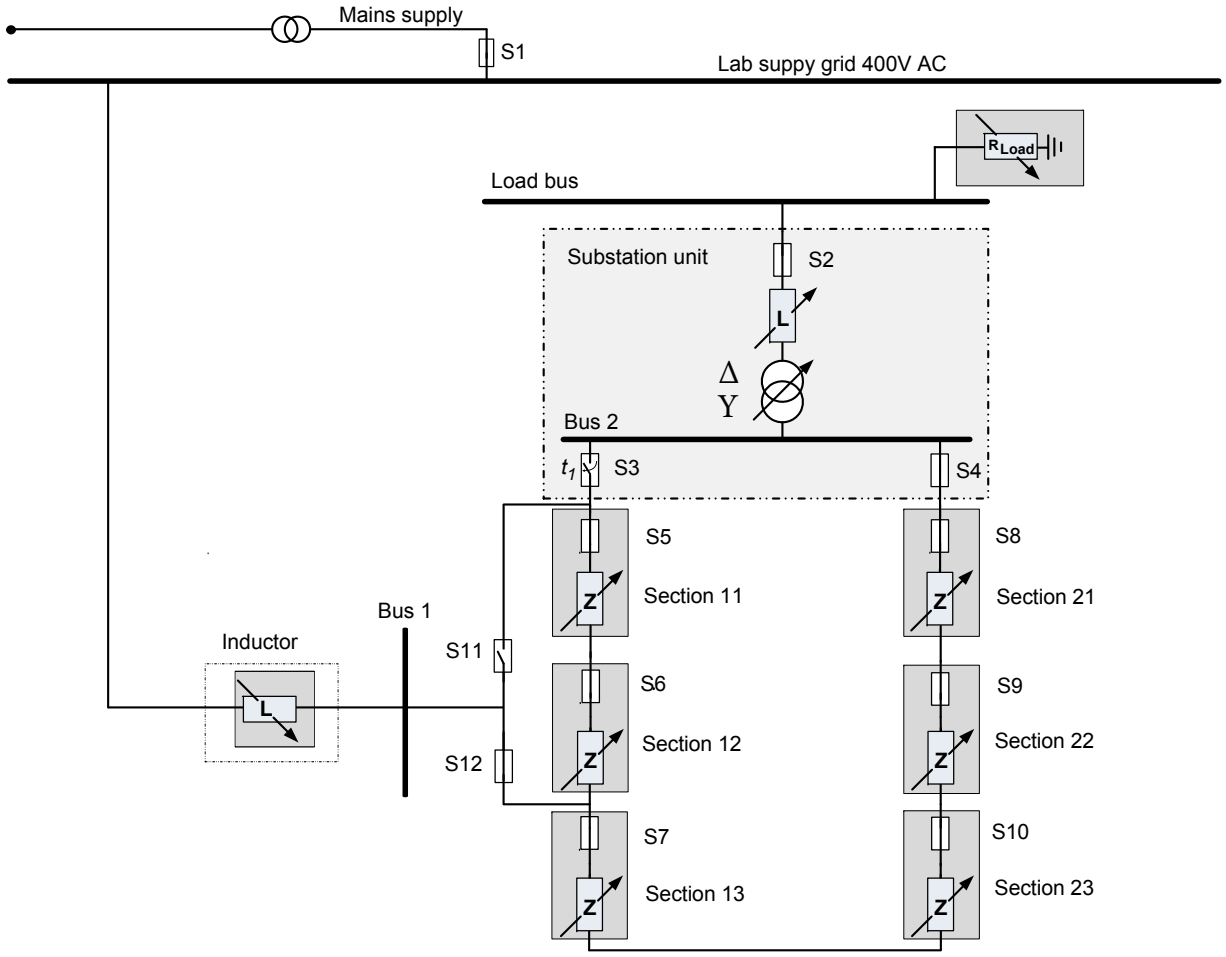


Figure 6.16: The laboratory setup configured to simulate a line trip.

Table 6.3: Switch connections and initial states.

| **Switch** | **Connection** | **Initial state** |
|---|---|---|
| S1 | Main supply | Closed |
| S2 | Transformer to load-bus | Closed |
| S3 | Feeder from line equivalent to substation | Closed |
| S4 | Feeder from line equivalent to substation | Closed |
| S5, S6, S7, S8, S9 & S10 | Distribution network sections | Closed |
| S11 | Connection point on the line equivalent | Open |
| S12 | Connection point on the line equivalent | Closed |

Before the line contingency the system impedance, $Z_{Sys}^{pre}$, can be estimated with background on these components parameters and a negligible short circuit impedance at the main supply, the system impedance is expected to be

$$Z_{Sys}^{pre} = X_{Inductor} + \frac{Z_{Line\,1} \cdot Z_{Line\,2}}{Z_{Line\,1} + Z_{Line\,2}} + Z_{Substation} \tag{6.8}$$

$$Z_{Sys}^{pre} = j0.31 + \frac{(2.78 + j3.12) \cdot (0.67 + j1.56)}{2.78 + j3.12 + 0.67 + j1.56} + 0.13 + j0.61\Omega = 0.71 + j2.00\Omega \tag{6.9}$$

$$|Z_{Sys}^{pre}| = \sqrt{0.71^2 + 2.00^2} = 2.12\Omega \tag{6.10}$$

After the line contingency, i.e. switch S3 is opened, the power system topology changes from conducting both $Z_{Line\,1}$ and $Z_{Line\,2}$ to only conducting through $Z_{Line\,1}$. This affects the system impedance as described in Section 3.3. The new system impedance $Z_{Sys}^{post}$, can be calculated

$$Z_{Sys}^{post} = X_{Inductor} + Z_{Line\,1} + Z_{Substation} \tag{6.11}$$

$$Z_{Sys}^{post} = j0.31 + 2.78 + j3.12 + 0.13 + j0.61\Omega = 2.91 + j4.04\Omega \tag{6.12}$$

$$|Z_{Sys}^{post}| = \sqrt{2.91^2 + 4.04^2} = 4.98\Omega \tag{6.13}$$

From Table. A.1 the minimum load impedance is estimated to be 5.6Ω which obviously are larger than the smallest possible system impedance in this configuration, meaning it is not expected to reach the maximum loadability limit in this experiment. The scenario starts with $Z_{Sys} = Z_{Sys}^{pre}$ and the load impedance gradually decreasing from infinite to 7.8Ω from $t = 0 - 500$ s. From $t = 500 - 1300$ s. the load impedance is varying between 7.8Ω and 7.4Ω, and in this time period the line contingency occurs at $t_1 = 830$ s. Tripping of the line causes the system impedance to become $Z_{Sys} = Z_{Sys}^{post}$. From time period $t = 1300 - 1500$ s the load impedance is decreased to a minimum value of 5.6Ω. After $t = 1500$ s the load power is at its maximum. To study the consequences of the line connection, the line is coupled back online at $t = 1580$ when the load impedance is at its minimum.

Table 6.4: Events of load demand and line trip/reconnect.

| Event | Time [s] |
|---|---|
| Load turned on and gradually decreased load impedance to 7.8Ω | 0-500 |
| Load impedance varying between 7.8Ω and 7.4Ω | 500-1300 |
| Line contingency | 830 |
| Load impedance gradually decreases from 7.4Ω to 5.6Ω | 1300-1500 |
| Maximum load power demand | 1500-1620 |
| Line reconnects to its original position | 1580 |

### 6.2.1 MATLAB Simulation

To simulate the theory of the indicators during a large disturbance described in Section 6.2, a simplified single-phase diagram is shown in Fig. 6.17. The main supply from the laboratory is represented as a constant voltage source with the reference angle $V\angle 0$, the inductor reactance $X_{Inductor}$, the flexible line equivalent divided into two parallel lines, $Z_{Line\,1}$ and $Z_{Line\,2}$. The substation unit $Z_{Substation}$. Current and voltage phasors, calculated by (6.18) and (6.17), are used to compute the indicators and the Thevenin impedance.

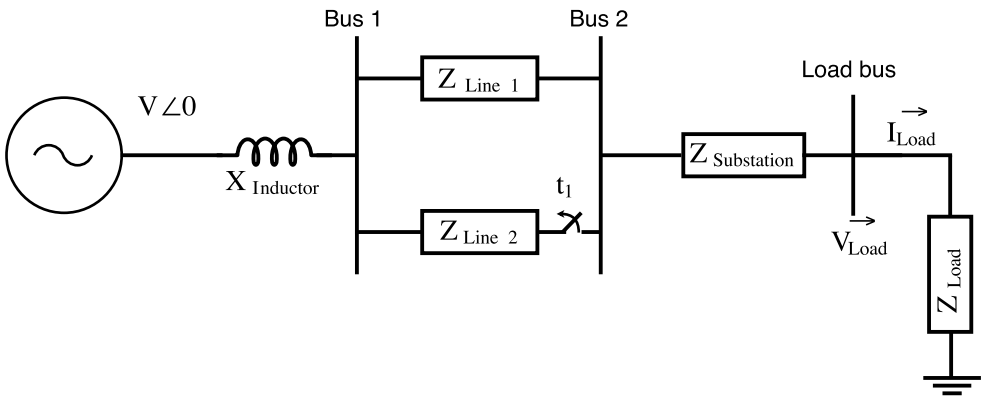


Figure 6.17: Simplified mode of the power system studied.

$$V = \frac{400}{\sqrt{3}} \angle 0 \tag{6.14}$$

$$Z_{Sys}^{pre} = X_{Inductor} + \frac{Z_{Line\,1} \cdot Z_{Line\,2}}{Z_{Line\,1} + Z_{Line\,2}} + Z_{Substation} \tag{6.15}$$

$$Z_{Sys}^{post} = X_{Inductor} + Z_{Line\,1} + Z_{Substation} \tag{6.16}$$

$$I_{Load} = \frac{V}{Z_{Sys}^{pre/post} + Z_{Load}} \tag{6.17}$$

$$V_{Load} = V - I_{Load} Z_{Sys}^{pre/post} \tag{6.18}$$

As seen in Fig. 6.18a, the load impedance is modeled as the scenario described in Section 6.2. The system impedance is modeled as an impedance set together from the system components parameters. Expressing the system impedance before the line trip as $Z_{Sys}^{pre}$, and after the line trip as $Z_{Sys}^{post}$.

The power-voltage characteristic is displayed in Fig. 6.18b, it shows that the power is increased while voltage is dropping, the line contingency occurs when the load voltage is 350 volts. The

voltage drops significantly and the corresponding power decreases as a result of the load is modeled as an impedance. The load now has a different operating situation and consequently a changed PV characteristic. While the load impedance decreases the load power in the weakened distribution grid gets almost to the nose point of the PV curve. The line connects back to the initial position at the lowest load impedance magnitude, decreasing the system impedance to $Z_{Sys}^{pre}$. The voltage rises severely with the resultant load power rise from roughly 10 kW to 20 kW.

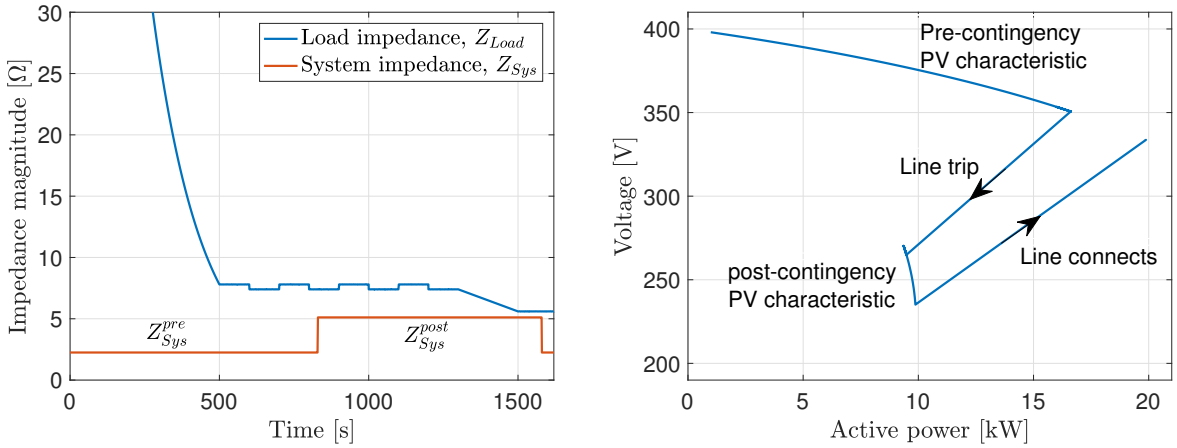


(a) Load and system impedance magnitude.

(b) PV characteristics.

Figure 6.18: Impedances and PV curves of the system during the MATLAB simulation.

Fig. 6.19 shows the indicators during the events, it can be seen that the indicators do not cross zero at any time, simply because the load impedance is larger than the system impedance, meaning that the nose point of the PV curve is not reached.

The S-YI and NLI are equal and positive at all times during these events and decreases when the load impedance decreases. S-ZI has its distinctive trajectory when the load is light, an increase in load power causes the S-ZI to decrease and reverses its direction. The line contingency triggers S-YI and NLI to drop and S-ZI to rise. The load power increase cause S-YI and NLI to go further down, S-ZI reacts by increasing. All indicators are close to indicating voltage instability, but as the load impedance is larger than the system impedance, the limit is not reached. When the line reconnects to its initial position the S-YI and NLI react by increasing in value, and S-ZI decreases.

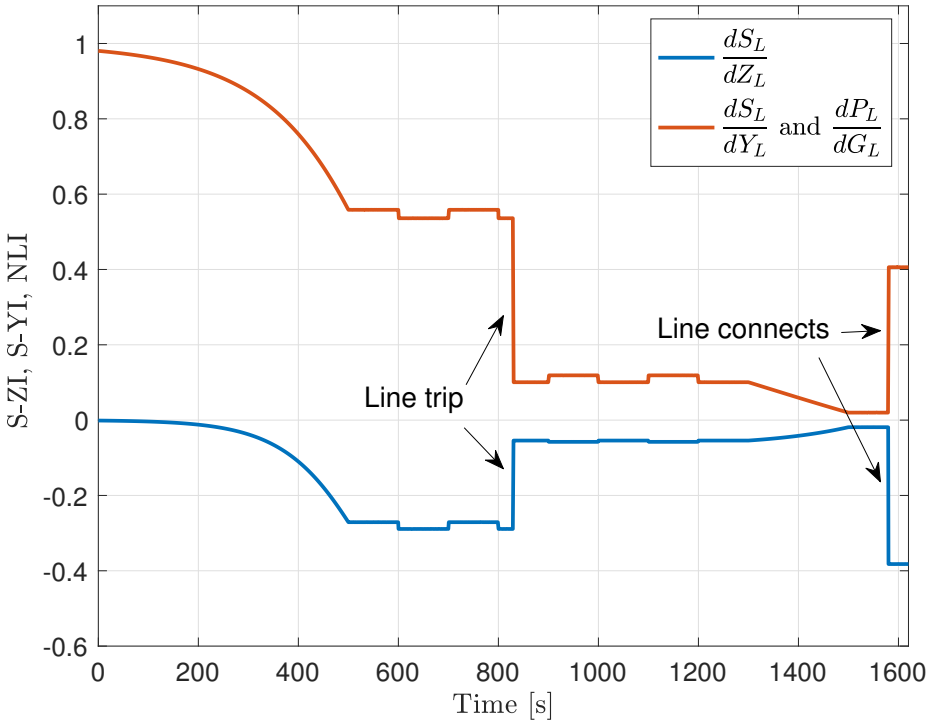


Figure 6.19: S-ZI versus time, the indicator clearly shows pattern compared to loading.

Fig. 6.20a shows a trajectory of the S-ZI versus load impedance magnitude. The load impedance is equal 7.4Ω when the line trips, the indicator then reacts accordingly by increasing. The indicator gets a new trajectory line as the operation premises have changed. The load impedance decreases before the line connects to its initial position and the indicator decreases appropriately. Fig. 6.20b depicts the S-YI and NLI as a function of conductance and admittance magnitude. Since the load is purely resistive the trajectories are identical for both indicators. It can be seen that the indicator, at the same value of conductance and admittance magnitude, drops significantly due to the line contingency and establishes at a new operation point. As the load admittance increases the indicators decrease and are close to the nose point of the PV curve as shown in Fig. 6.18b. The connection of the line results in an increase of the S-YI and NLI indicators as the system impedance decreases. Fig. 6.21 shows the load impedance and the Thevenin impedance magnitudes obtained from S-Z and S-Y method described in Section 4.3.2 and Section 4.4.2. The Thevenin impedance computed from S-Z method and S-Y method are in this MATLAB simulation equal to each other. As can be seen, the Thevenin impedance is approximately equal the system impedance $Z_{Sys}^{pre/post}$, and follows the events in terms of time.

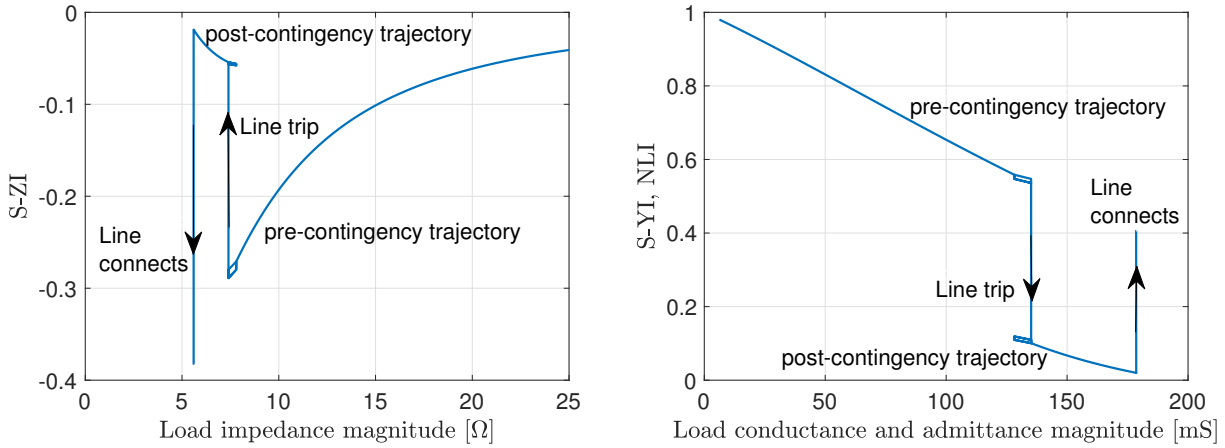


(a) S-Z indicator versus load impedance.

(b) SY-I and NLI versus conductance and admittance magnitude.

Figure 6.20: Indicators versus loading of the system during MATLAB simulation.

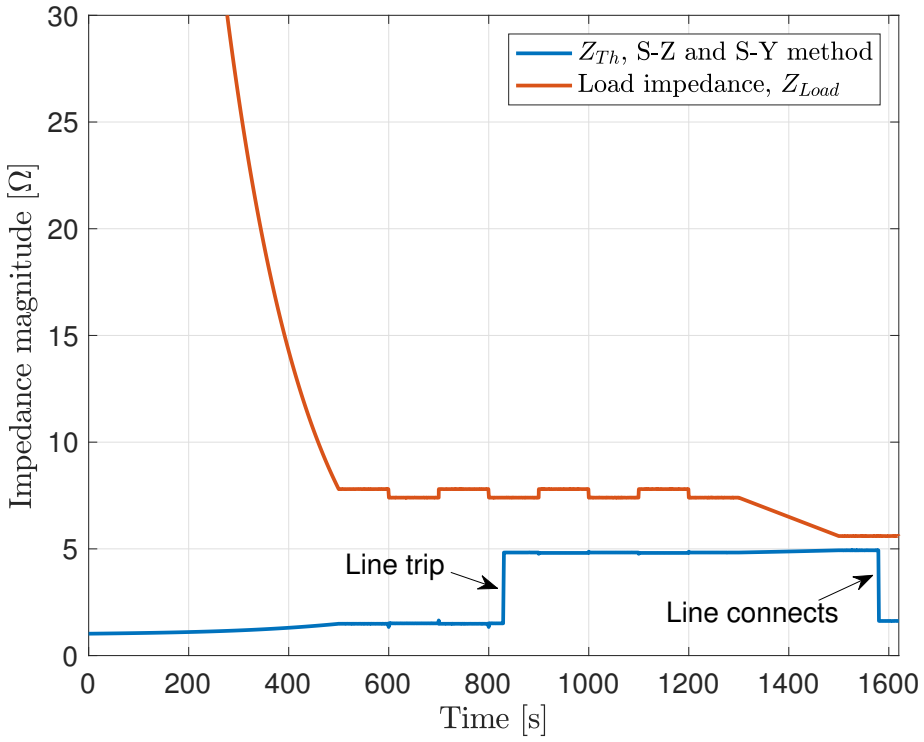


Figure 6.21: Thevenin impedance seen from the load bus.

### 6.2.2 Laboratory Experiment

If the power system is exposed to a large disturbance, its operation condition changes. In order to study the indicators and the S-Z and S-Y methods during a large disturbance, a line contingency is done in a laboratory experiment. The events are as described in Section 6.2 and listed in table 6.4. Fig. 6.22a shows the measurements of voltage and current magnitudes during the laboratory test. It can be seen that the line contingency has a large influence on the current and voltage, the voltage drops from 340 volts to 260 volts. As a consequence of the line trip, the maximum power transfer limit decreases as described in Section 3.3.

As seen in Fig. 6.22b the active power drops from 15.90 kW to 8.98 kW when the line trip. The PV characteristics plotted in Fig. 6.23 shows the power decreasing when the disturbance occurs. A new operating state is established and at this point a new PV characteristic is set. The PV curve is now much closer to the nose point than before the line disconnect. As the load power is increasing, the increase in current makes the voltage drop across the system impedance larger, giving a smaller voltage at the load bus. When the line is connected back to its initial position, the load power goes from 9.52 kW to 19.10 kW.

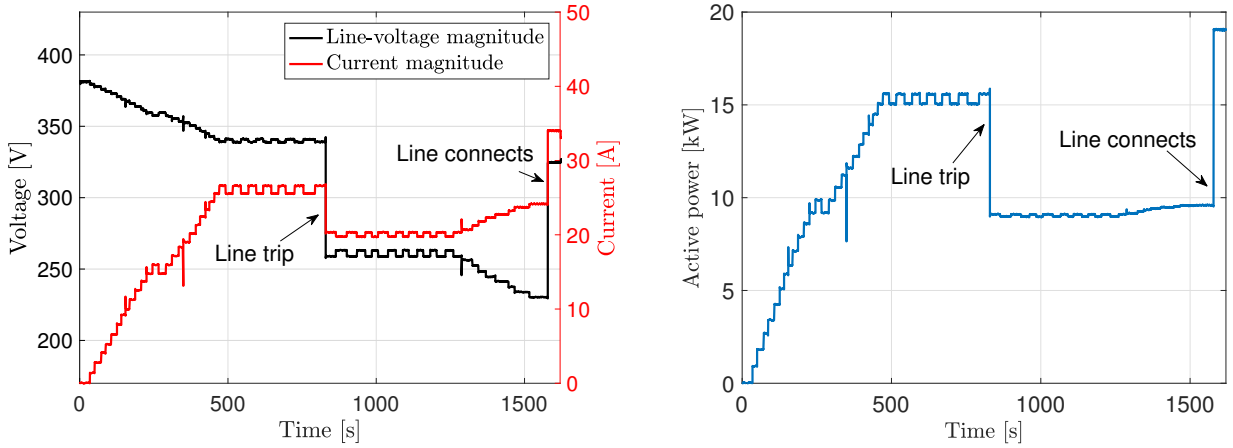


(a) Voltage and current magnitudes versus time.

(b) Active power versus time.

Figure 6.22: Measurements done during the experiment with a trip of a line.

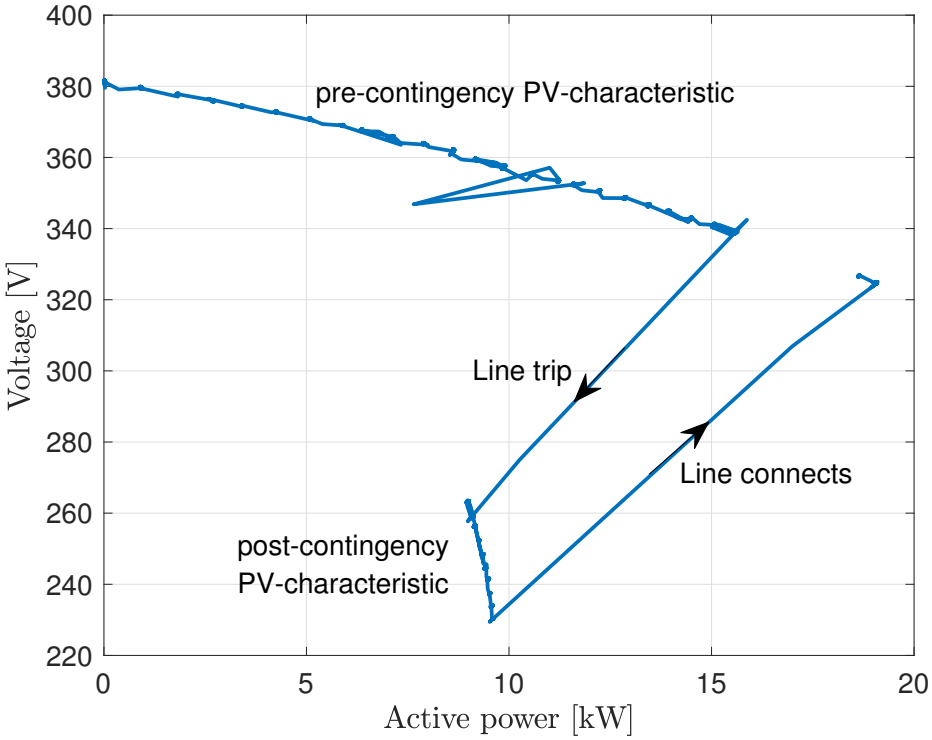


Figure 6.23: PV characteristics.

Fig. 6.24a shows the S-Z sensitivity indicator during the scenario. The indicator is negative before the contingency, with its distinctive trajectory. As the load impedance decreases (load power increase), the indicator decreases. The line trip causes the indicator to burst positive, having its zero crossing at $t = 800$ s and $t = 880$ s, indicating voltage instability for 80 s. It is noted that the indicator shows a pattern from the MATLAB simulation done in Section 6.2.1. As the S-ZI is more negative before the line contingency $S-ZI = -0.8$, then after some time after the line trip, $S-ZI = -0.2$. This indicates that the distance is shorter due to voltage instability after the line trip. The responses of the indicator are earlier than the actual events, for example the line trip happens at $t = 830$ s, the indicator has its first zero crossing at $t = 800$ s. The load increase after the disconnection of the line is also readable from the plot, at $t = 1000$ s the $S-ZI = -0.20$ and after the load increase at $t = 1450$ s the $S-ZI = -0.14$. After reconnecting the line, the indicator decreases as expected.

Fig. 6.24b shows the S-ZI indicator versus the load impedance magnitude. The S-ZI has two trajectories, before and after line trip. The line trips when the load impedance is 7.4Ω, the indi-

cator then stabilizes at a new operating point $S-ZI = -0.2$. When the load impedance decreases the indicator has a slight increase moving towards the nose point. The S-Z sensitivity indicator decreases as a result of the line connecting back on-line.

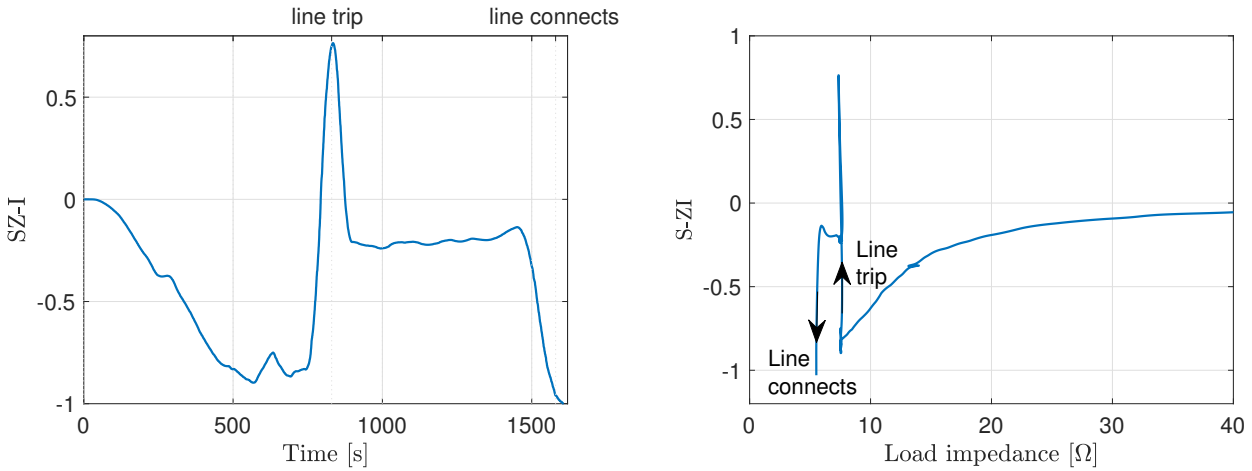


(a) S-Z sensitivity indicator versus time.

(b) S-ZI verus load impedance magnitude.

Figure 6.24: S-ZI during the experiment.

S-Y sensitivity indicator versus time is plotted in Fig. 6.25a. The indicator starts at its maximum when the load is light and decreases as the load power increases. The line contingency causes a dip in the indicator, and has its zero crossing at $t = 800$ s, slightly before the line trip happens. S-YI turns positive again at $t = 880$ and has new operating point roughly at $S-YI = 0.1$. Meaning the S-YI indicates voltage instability for 80 s. When the load impedance decreases the indicator responds by decreasing as expected and has a short distance to indicating voltage instability with $S-YI = 0.03$ at $t = 1450$ s. When the line connects the indicator bursts positive.

As seen in Fig. 6.25b the indicator, S-YI is computed versus the load admittance magnitude. it clearly shows a pattern as in Fig. 4.6a as expected. The large disturbance causes the indicator to be negative at the loading of 0.13 S, corresponding to $Z_{Load} = 7.70\Omega$. However, the indicator establishes a new positive operating point after the dip. When increasing the load power (increasing admittance), the indicator decreases. As the line connects back on-line the S-YI increases as expected.

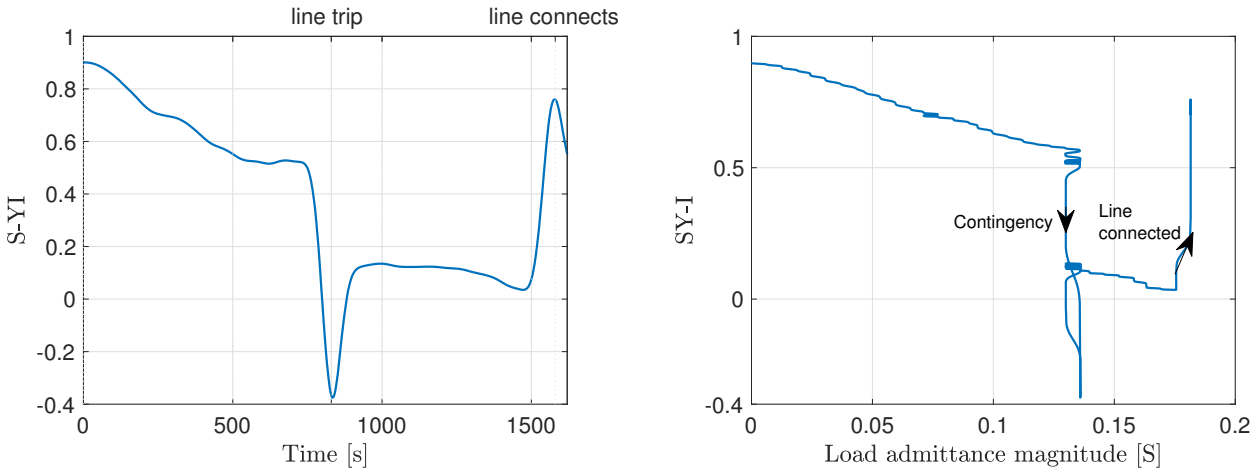


(a) S-Y sensitivity indicator versus time.

(b) S-YI verus load admittance magnitude.

Figure 6.25: S-YI during the experiment.

Fig. 6.26a shows the NLI indicator during the events described in Section 6.2. The indicator has, as expected, the same pattern as the S-YI as a result of the resistive load. This causes Fig. 6.26b to show the same pattern as Fig. 6.25b. As the load impedance decrease, the indicator decreases. The line contingency causes the indicator to burst negative at $t = 800$ s, then positive at $t = 880$, indicating voltage instability for 80 s. A new operating point is established after the line trip at $NLI = 0.15$, the indicator decreases further when the load impedance decreases and have a short distance to indicate that the maximum power transfer limit is reached when the load impedance is minimum. The indicator increases when the line is reconnected.

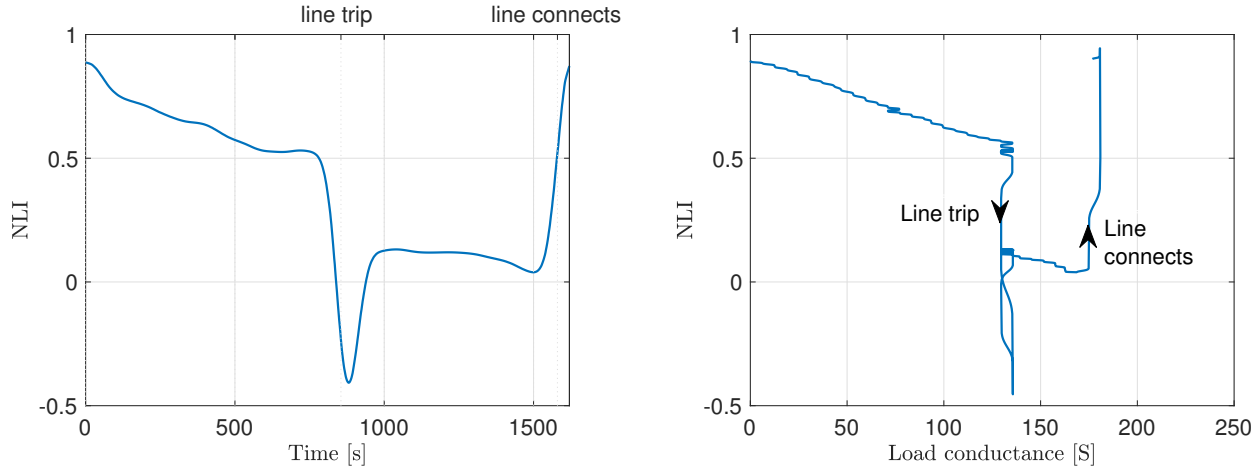


(a) NLI indicator versus time.

(b) NLI versus load conductance.

Figure 6.26: NLI during the experiment.

By applying the S-Z and S-Y methods the Thevenin impedance is estimated for this experiment. Fig. 6.27a shows the load impedance magnitude together with the two Thevenin impedances. The Thevenin impedance is very associated to the S-ZI and S-YI indicators, and as a result of the line contingency, it can be seen that the Thevenin impedance has a larger magnitude than the load impedance at $t = 750$ s. The Thevenin impedance establishes itself to the new operating conditions. The magnitude of the Thevenin impedance before the line contingency is approximate $Z_{Th} = 2\Omega$ and after it is $Z_{Th} = 5\Omega$. When the line connects back on-line the Thevenin impedance reacts by decreasing as expected. The Thevenin impedance is comparable with both $Z_{Sys}^{pre}$ before the line trip and $Z_{Sys}^{post}$ after the line trip. However, the large peak in the Thevenin impedance when the line trip is not recognizable from the laboratory setup.

Fig. 6.27b shows the estimated maximum power from both S-Z and S-Y method. The load power is never above the estimated maximum power. The power margin has large variations before the line contingency, and as expected, the power margin drops after the line trip and the transfer capacity is reduced. When the line reconnects, the estimated maximum power increases.

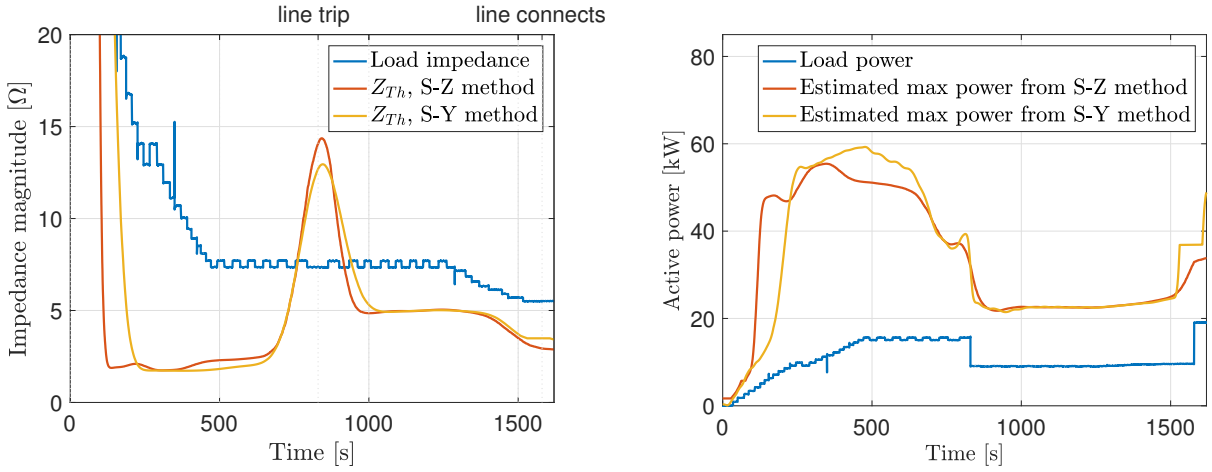


(a) Impedance magnitudes versus time.

(b) Estimated maximum power and load power

Figure 6.27: Thevenin impedances and the corresponding maximum power.

In normal operation the Fig. 6.24b is unavailable unless an occurrence of the maximum power transfer condition is fulfilled. To have an estimate of the curve, one can plot the trajectory of S-ZI versus the load impedance magnitude in advance by using (4.12) from Section 4.1. The Thevenin impedance is set equal $Z_{Sys}^{post}$, and the red dot is the S-ZI at $t = 1200$ s, the load

impedance is at this time 7.4Ω, and as red dot is located along the trajectory, the estimation of the Thevenin impedance is correct. If the estimation of the Thevenin impedance was inaccurate, the red dot would not be located along the curve. This feature is used as a measure to validate the estimation of the Thevenin impedance.

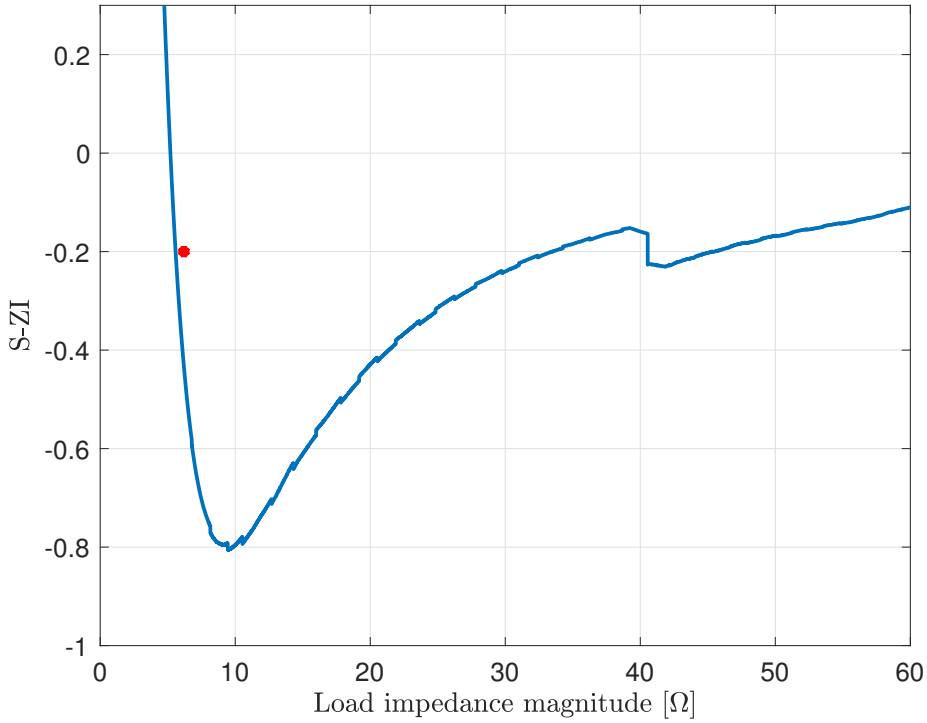


Figure 6.28: S-ZI versus load impedance magnitude.

### 6.2.3 Discussion

The indicators show a realistic motion compared to the loading of the system and were closer to their stability limit after line disconnection, this is because the line trip made the system significantly weaker. This illustrates that the indicators can reliably assess the situation of the network. The exception was when the line contingency happened, the indicators showed abnormal values compared to the loading of the system. A severe decrease in apparent power follows with the line contingency. As a result of this, the indicator has its zero crossing before stabilizing as the new operating conditions are set. For this experiment the active load power is equal to the load apparent power since the load is completely resistive, therefore the change in active power is equal the change in apparent power. NLI has consequently the same pattern as the S-Y sensi-

tivity indicator as a result of the large spikes in the indicator values.

The observed spikes correspond to the slashes in the PV curves as the system shifts from one state to another, and is a result of the indicators being described for steady-state conditions, while the change between two stable operating points is a transient occasion.

When looking at the zero crossing of the indicators, indicating voltage instability from $t$ = 800 s to $t$ = 880 s, however, the line trip happened at $t$ = 830 s. The reason is that in this computation, the moving average filter used samples from both the past and the future to compute data points (this is only possible with offline measurements). Resulting in an inaccurate indication and would not work in real-time as the indicators cannot foresee the future. This could be solved by considering only samples from the past of the measurements and remove measurements that are above a certain value to remove transients. Another filtering improvement would be to have one short-term indicator and one long-term indicator. Where the short-term uses fewer samples and consider transients, being more suitable for large disturbances. Long-term indicator considers more samples and not transient events, being more suitable for load variations.

Estimation of the Thevenin impedance from the S-Z and S-Y method was comparable to the calculated system impedance ($Z_{Sys}^{pre/post}$) and could be used as measures of temporary strength of the network. However, the indicators S-ZI and S-YI affects the estimation of the Thevenin impedance significantly; as the indicators signify voltage instability, the Thevenin impedance is larger than the load impedance. This is obviously not the case and an improvement on the filtering would enhance the Thevenin impedance in this simulation.

With the Thevenin impedance, load current and voltage, the maximum loadability is estimated by (4.3). The estimated maximum loadability is largely influenced by the Thevenin impedance, a small error of the Thevenin impedance can lead to a large variation of the estimated maximum power. Therefore, cannot measure the ultimate limit of the system transfer capacity.

It is important to remember that the computations presented in this thesis are done off-line, the PMU data from the laboratory experiments are processed and reviewed before presenting the various plots. In real-time computations this is not a feasible option.

# Chapter 7

# Conclusion and further work

## 7.1 Conclusion

All of the three presented indicators had excellent performance under small disturbances, in this study the small disturbance was increased load demand. The maximum loadability limit was reached in the case described in Section 6.1, and the indicators were able to detect, with an acceptable time deviation, its maximum power transfer often referred to as the tip of the nose point of a PV curve. The indicators determine whether the system is on the stable upper half or the unstable lower half of the PV curve. All the indicators follow the distinctive trajectories described in Chapter 4, and are equal to zero when the load power is at its maximum value.

When the laboratory power system was exposed to a large disturbance the results of the indicators gave an incorrect view of the system. As the line tripped the indicators signified voltage instability, which is equivalent to the lower part of the PV curve. This is a result of a very high change in power, due to the large disturbance. It is possible to filter out the large changes to avoid the misleading indication. The filter used samples from the past and the future to calculate values used in plots, this would not work in real-time as the indicators cannot foresee the future. Particularly after being subjected to a large disturbance this resulted in giving misleading voltage stability indicators. Indicating voltage instability for 80 s as a consequence of the transient occurrence that comes with a line contingency. This could be corrected by considering only samples from the past and remove data that are above a certain value to eliminate tran-

sients. Another improvement could be to have one short-term indicator and one long-term indicator. The short-term apply fewer samples and consider transient events, being more suitable for large disturbances. Long-term indicator considers more samples and not transient events, being more appropriate for load variations.

Estimation of the Thevenin impedance from the S-Z and S-Y method was corresponding to the calculated system impedance ($Z_{Sys}$) under both experiments and could be used as measures of temporary strength of the network. However, the Thevenin impedance is strongly influenced by the S-YI and S-ZI. Thus, computations of the Thevenin impedance should be done by utilizing the suggested long-term indicators.

The estimated maximum loadability is largely influenced by the Thevenin impedance, a small error of the Thevenin impedance can lead to a large variation of the estimated maximum power. Therefore, the estimated maximum transfer limit cannot measure the ultimate limit of the system transfer capacity.

Through MATLAB simulations and laboratory experiments, the indicators follow the predefined trajectories. The S-ZI and S-YI have verified the Thevenin impedance seen at the load bus. Given a Thevenin impedance, it is possible to draw a trajectory of the S-ZI and S-YI versus the load impedance magnitude and load admittance magnitude. If the Thevenin impedance is correctly estimated the resultant S-ZI and S-YI values appear in the S-ZI and S-YI trajectory.

Implementation of these methods and indicators requires PMU measurements of the load voltage and current, and do not need any topology information. This makes it viable for practical implementations in power systems to have an online voltage stability monitoring. It is sufficiently verified trough simulations and laboratory experiments that the methods and indicators are suitable for voltage stability assessment in real-time.

## 7.2 Recommendations for Further Work

There are various ways to continue the work of this thesis. First, the theoretical basis of the indicators and estimation of the Thevenin impedance should be evaluated.

In this thesis the load is a resistive constant impedance, the results of S-YI and NLI was then comparable. Their validity should be proved in more test in terms of different power factors and loading mechanisms as load modeling is of great importance. Additionally, a PMU could be placed to monitor the voltage phasor at the main supply bus. The Thevenin equivalent would be known and could be compared to the estimated Thevenin impedance seen from the load bus to validate the Thevenin impedance.

The Thevenin impedance in this laboratory work has large variations when the load impedance is large (load power is low). The cause could be that there are very small changes in the sensitivity trajectories from S-Z and S-Y method when the load is light. This is obviously a limitation of the estimation of the Thevenin impedance and could be studied.

The robustness of the indicators needs to be further studied. In a real power system, disturbances occur, and the system is never completely balanced. As seen in Section 6.2 the indicators in this thesis are greatly affected by the line contingency, a suggestion is to improve the filtering of the indicators as discussed in Section 6.2.3.

New LIVES Index focuses on active power and the apparent load conductance at a measured bus. It would be interesting to have a laboratory experiment where the PMU is located at a transmission bus, measuring the effect of line losses.

# Bibliography


[1] J. R. Bumby J. Machowski, J. W. Bialek. *Power System Dynamics, Stability and Control.* John Wiley and Sons Ltd, 2008.

[2] Kjetil Uhlen. Smart transmission grids operation and control. http://www.ntnu.edu/documents/1263763591/1269572391/NTNU-ProSmart-seminar-May2016-Kjetil.pdf/3687a728-9dde-415f-a796-96b044d9f848.

[3] Statnett. Årsstatistikk 2015 driftsforstyrrelser og feil i 33-420 kv-nettet. http://www.statnett.no/Global/Dokumenter/Kraftsystemet/Systemansvar/Feilstatistikk/%C3%85rsstatistikk%202015%2033-420%20kV.pdf.

[4] Continental europe operation handbook - glossary. https://www.entsoe.eu/fileadmin/user_upload/_library/publications/entsoe/Operation_Handbook/glossary_v22.pdf, 2004.

[5] P. Kundur, J. Paserba, V. Ajjarapu, G. Andersson, A. Bose, C. Canizares, N. Hatziargyriou, D. Hill, A. Stankovic, C. Taylor, T. Van Cutsem, and V. Vittal. Definition and classification of power system stability IEEE/CIGRE joint task force on stability terms and definitions. *IEEE Transactions on Power Systems*, 19(3):1387–1401, Aug 2004.

[6] P. Kundur. *Power System Stability and Control.* New York: McGrawHill, 1994.

[7] IEEE standard for synchrophasors for power systems. *IEEE Std C37.118-2005 (Revision of IEEE Std 1344-1995)*, pages 01–57, 2006.

[8] Philip Overholt B. M. Kjetil Uhlen and O. Valentine. Synchrophasor applications for wide area monitoring and control. *ISGAN annex 6 power T&D systems*, 2016.

[9] T. Van Cutsem and C. Vournas. *Voltage Stability of Electric Power Systems*. Norwell, MA: Kluwer, 1998.

[10] Dinh Thuc Duong. *Online Voltage Stability Monitoring and Coordinated Secondary Voltage Control*. PhD thesis, NTNU, 2016.

[11] Load representation for dynamic performance analysis [of power systems]. *IEEE Transactions on Power Systems*, 8(2):472–482, May 1993.

[12] K. Vu, M. M. Begovic, D. Novosel, and M. M. Saha. Use of local measurements to estimate voltage-stability margin. In *Proceedings of the 20th International Conference on Power Industry Computer Applications*, pages 318–323, May 1997.

[13] M. Begovic, B. Milosevic, and D. Novosel. A novel method for voltage instability protection. In *Proceedings of the 35th Annual Hawaii International Conference on System Sciences*, pages 802–811, Jan 2002.

[14] Y. Wang, I. R. Pordanjani, W. Li, W. Xu, T. Chen, E. Vaahedi, and J. Gurney. Voltage stability monitoring based on the concept of coupled single-port circuit. *IEEE Transactions on Power Systems*, 26(4):2154–2163, Nov 2011.

[15] A. Wiszniewski. New criteria of voltage stability margin for the purpose of load shedding. *IEEE Transactions on Power Delivery*, 22(3):1367–1371, July 2007.

[16] C. D. Vournas, C. Lambrou, and P. Mandoulidis. Voltage stability monitoring from a transmission bus pmu. *IEEE Transactions on Power Systems*, PP(99):1–1, 2016.

[17] Astrid Petterteig. Report - distribution network laboratory model. Technical report, SINTEF Energy, 2011.

[18] Hans Kristian Hansen. Animations of the laboratory work results. https://www.dropbox.com/sh/giddt4asrcwecrx/AAC1tq5cqW-YnvoHh_uGc3JKa?dl=0.

# Appendix A

# Laboratory Model

Following laboratory model used in this thesis. [17]

## A.1 Coil

The variable inductor is shown in Fig. A.1.

Figure A.1: Variable inductor.

## A.2 Line Equivalent Resistances

The following next two pages was obtained from a report from SINTEF. Measurements and documentation where made on the line equivalent model seen in Fig. A.2. [17]

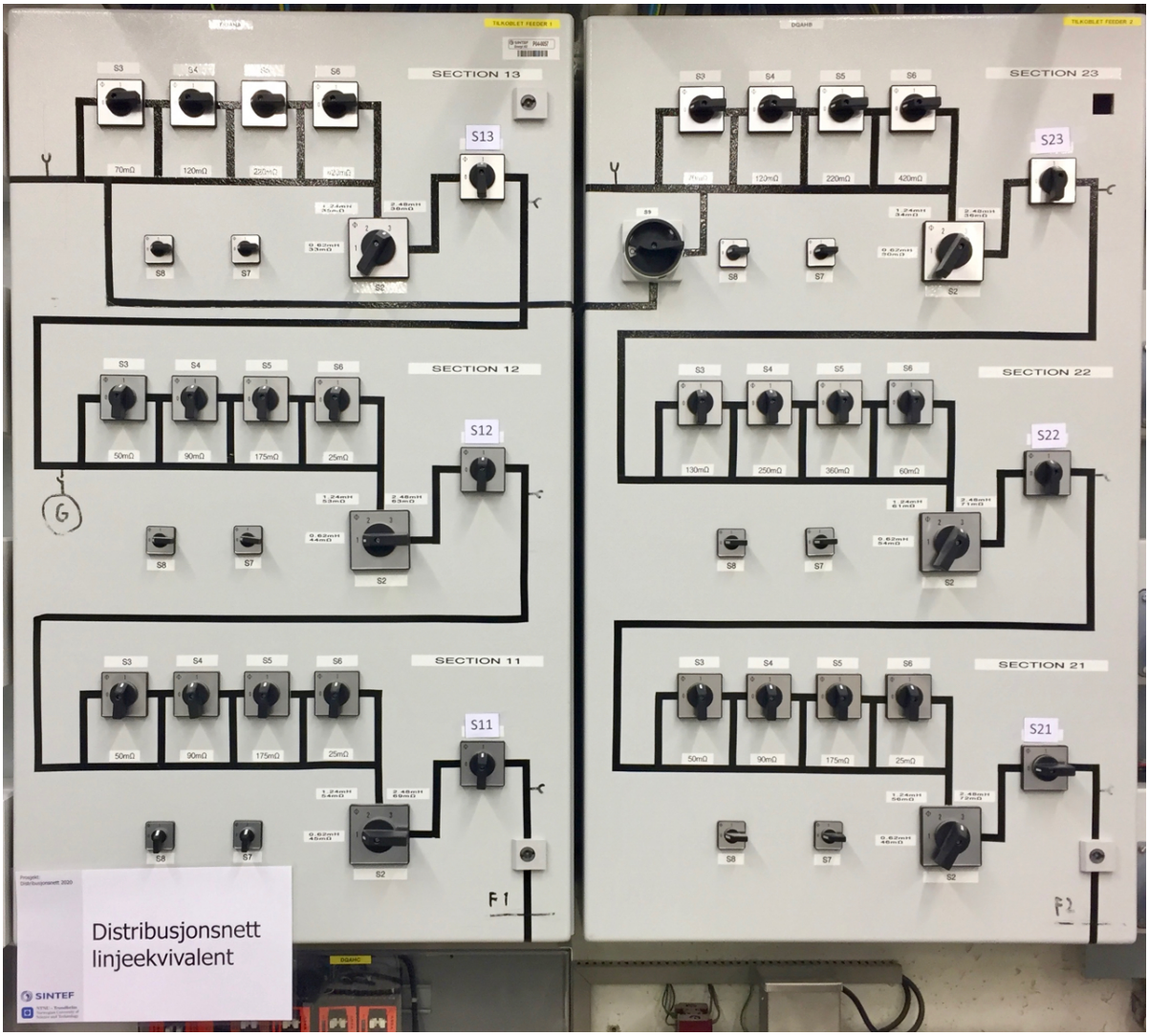


Figure A.2: Network model.

SINTEF

## Measured resistance values (resistors only)

The final resistance values have been checked by measurements done inside the switch cabinet. The resistance values measured are presented below. Note that the order of the resistance parts ($R_I$ – $R_{IV}$) have changed compared to the plans (B.1). This and the uncertainties of the cable resistances and the inaccuracy due to physical placement of contacts cause the final resistances to deviate from the planned. There will also be some unbalance between phases.

**Resistance values including cable resistances:**

| Section 11 | R | S | T | Type (ref. B.1) |
|---|---|---|---|---|
| S6 open | 22-24 mΩ | 22-24 mΩ | 22-24 mΩ | $R_I$ |
| S5 open | 175 mΩ | 177 mΩ | 177 mΩ | $R_{IV}$ |
| S4 open | 89 mΩ | 89 mΩ | 88 mΩ | $R_{III}$ |
| S3 open | 46 mΩ | 47 mΩ | 48 mΩ | $R_{II}$ |

| Section 12 | R | S | T | Type |
|---|---|---|---|---|
| S6 open | 23 mΩ | 24 mΩ | 25 mΩ | $R_I$ |
| S5 open | 169 mΩ | 174 mΩ | 176 mΩ | $R_{IV}$ |
| S4 open | 86 mΩ | 86 mΩ | 87 mΩ | $R_{III}$ |
| S3 open | 48 mΩ | 50 mΩ | 51 mΩ | $R_{II}$ |

| Section 13 | R | S | T | Type |
|---|---|---|---|---|
| S6 open | 419 mΩ | 416 mΩ | 423 mΩ | $R_{IV}$ |
| S5 open | 215 mΩ | 208 mΩ | 225 mΩ | $R_{III}$ |
| S4 open | 123 mΩ | 118 mΩ | 118 mΩ | $R_{II}$ |
| S3 open | 77 mΩ | 68 mΩ | 75 mΩ | $R_I$ |

| Section 21 | R | S | T | Type |
|---|---|---|---|---|
| S6 open | 24 mΩ | 27 mΩ | 26 mΩ | $R_I$ |
| S5 open | 173 mΩ | 175 mΩ | 173 mΩ | $R_{IV}$ |
| S4 open | 89 mΩ | 88 mΩ | 88 mΩ | $R_{III}$ |
| S3 open | 46 mΩ | 48 mΩ | 49 mΩ | $R_{II}$ |

| Section 22 | R | S | T | Type |
|---|---|---|---|---|
| S6 open | 59 mΩ | ~ 59 mΩ | ~ 59 mΩ | $R_I$ |
| S5 open | 364 mΩ | 367 mΩ | 364 mΩ | $R_{IV}$ |
| S4 open | 246 mΩ | 247 mΩ | 248 mΩ | $R_{III}$ |
| S3 open | 128 mΩ | 128 mΩ | 133 mΩ | $R_{II}$ |

| Section 23 | R | S | T | Type |
|---|---|---|---|---|
| S6 open | 421 mΩ | 423 mΩ | 424 mΩ | $R_{IV}$ |
| S5 open | 220 mΩ | 207 mΩ | 212 mΩ | $R_{III}$ |
| S4 open | 116 mΩ | 116 mΩ | 117 mΩ | $R_{II}$ |
| S3 open | 68 mΩ | 71 mΩ | 68 mΩ | $R_I$ |

SINTEF

## Breaker status and measured line equivalent resistance values

| Switch setting, Equivalent length | L1: 2km | L2: 4 km | L3: 8 km |
|---|---|---|---|
| Inductance, (50 Hz Reactance) | 0,6 mH (188 mOhm) | 1,24 mH (390 mOhm | 2,48 mH (780 mOhm) |

Breaker status and line section resistance for the different equivalent line section.

| Equivalent 22 kV line dimension | "Ideal" resistance (wanted value) | Physical resistance - resistor & coil (measured values) | Section 11 & Section 21 (400 A coil) | | | | | | | | | | | |
|---|---|---|---|---|---|---|---|---|---|---|---|---|---|---|
| | | | 2km | | | | 4 km | | | | 8 km | | | |
| | | | S3 | S4 | S5 | S6 | S3 | S4 | S5 | S6 | S3 | S4 | S5 | S6 |
| **240 mm²** | 42, 85, 169 mΩ | **46, 94, 188 mΩ** | I | I | I | I | 0 | I | I | I | 0 | 0 | I | 0 |
| **150 mm²** | 67, 135, 269 mΩ | **59, 134, 270 mΩ** | I | I | I | 0 | I | 0 | I | I | 0 | I | 0 | I |
| **120 mm²** | 84, 168, 336 mΩ | **84, 171, 326 mΩ** | 0 | I | I | I | 0 | 0 | I | 0 | 0 | 0 | 0 | 0 |
| **95 mm²** | 106, 213, 425 mΩ | **97, 217 mΩ** | 0 | I | I | 0 | I | I | 0 | I | | | | |
| **70 mm²** | 143, 286, 572 mΩ | **150, 284 mΩ** | 0 | 0 | I | I | I | 0 | 0 | 0 | | | | |
| **50 mm²** | 200, 400, 799 mΩ | **208 mΩ** | I | I | 0 | I | | | | | | | | |
| **25 mm²** | 401, 803, 1605 mΩ | | | | | | | | | | | | | |

| Equivalent 22 kV line dimension | "Ideal" resistance (wanted value) | Physical resistance - resistor & coil (measured values) | Section 12 (200 A coil) | | | | | | | | | | | |
|---|---|---|---|---|---|---|---|---|---|---|---|---|---|---|
| | | | 2km | | | | 4 km | | | | 8 km | | | |
| | | | S3 | S4 | S5 | S6 | S3 | S4 | S5 | S6 | S3 | S4 | S5 | S6 |
| **240 mm²** | 42, 85, 169 mΩ | **44, 94, 179 mΩ** | I | I | I | I | 0 | I | I | I | 0 | 0 | I | 0 |
| **150 mm²** | 67, 135, 269 mΩ | **55, 140, 263 mΩ** | I | I | I | 0 | I | 0 | I | 0 | 0 | I | 0 | 0 |
| **120 mm²** | 84, 168, 336 mΩ | **83 , 170, 315 mΩ** | 0 | I | I | I | 0 | 0 | I | 0 | 0 | 0 | 0 | 0 |
| **95 mm²** | 106, 213, 425 mΩ | **119, 214, mΩ** | I | 0 | I | I | I | I | 0 | 0 | | | | |
| **70 mm²** | 143, 286, 572 mΩ | **148, 312 mΩ** | 0 | 0 | I | I | 0 | 0 | 0 | I | | | | |
| **50 mm²** | 200, 400, 799 mΩ | **201 mΩ** | I | I | 0 | I | | | | | | | | |
| **25 mm²** | 401, 803, 1605 mΩ | | | | | | | | | | | | | |

| Equivalent 22 kV line dimension | "Ideal" resistance (wanted value) | Physical resistance - resistor & coil (measured values) | Section 22 (200 A coil) | | | | | | | | | | | |
|---|---|---|---|---|---|---|---|---|---|---|---|---|---|---|
| | | | 2km | | | | 4 km | | | | 8 km | | | |
| | | | S3 | S4 | S5 | S6 | S3 | S4 | S5 | S6 | S3 | S4 | S5 | S6 |
| **240 mm²** | 42, 85, 169 mΩ | **54, 61, 191, mΩ** | I | I | I | I | I | I | I | I | 0 | I | I | I |
| **150 mm²** | 67, 135, 269 mΩ | **54, 108, 238 mΩ** | I | I | I | I | I | I | I | 0 | 0 | I | I | 0 |
| **120 mm²** | 84, 168, 336 mΩ | **101, 181, 353 mΩ** | I | I | I | 0 | 0 | I | I | I | I | 0 | I | 0 |
| **95 mm²** | 106, 213, 425 mΩ | **101, 228, 424 mΩ** | I | I | I | 0 | 0 | I | I | 0 | I | I | 0 | I |
| **70 mm²** | 143, 286, 572 mΩ | **174, 296, 578 mΩ** | 0 | I | I | I | I | 0 | I | I | 0 | I | 0 | 0 |
| **50 mm²** | 200, 400, 799 mΩ | **221, 414,781 mΩ** | 0 | I | I | 0 | I | I | 0 | I | 0 | 0 | 0 | 0 |
| **25 mm²** | 401, 803, 1605 mΩ | **407, 771 mΩ** | I | I | 0 | I | 0 | 0 | 0 | 0 | | | | |

| Equivalent 22 kV line dimension | "Ideal" resistance (wanted value) | Physical resistance - resistor & coil (measured values) | Section 13 & Section 23 (100 A coil) | | | | | | | | | | | |
|---|---|---|---|---|---|---|---|---|---|---|---|---|---|---|
| | | | 2km | | | | 4 km | | | | 8 km | | | |
| | | | S3 | S4 | S5 | S6 | S3 | S4 | S5 | S6 | S3 | S4 | S5 | S6 |
| **240 mm²** | 42, 85, 169 mΩ | **30, 94, 186 mΩ** | I | I | I | I | 0 | I | I | I | 0 | 0 | I | I |
| **150 mm²** | 67, 135, 269 mΩ | **90, 139,290 mΩ** | 0 | I | I | I | I | 0 | I | I | 0 | I | 0 | I |
| **120 mm²** | 84, 168, 336 mΩ | **90, 139, 365 mΩ** | 0 | I | I | I | I | 0 | I | I | 0 | 0 | 0 | I |
| **95 mm²** | 106, 213, 425 mΩ | **90, 229, 439 mΩ** | 0 | I | I | I | I | I | 0 | I | I | I | I | 0 |
| **70 mm²** | 143, 286, 572 mΩ | **135, 287, 590 mΩ** | I | 0 | I | I | 0 | I | 0 | I | 0 | 0 | I | 0 |
| **50 mm²** | 200, 400, 799 mΩ | **225, 437, 751 mΩ** | I | I | 0 | I | I | I | I | 0 | 0 | 0 | 0 | 0 |
| **25 mm²** | 401, 803, 1605 mΩ | **434, 748 mΩ** | I | I | I | 0 | 0 | 0 | 0 | 0 | | | | |

## A.3 Substation

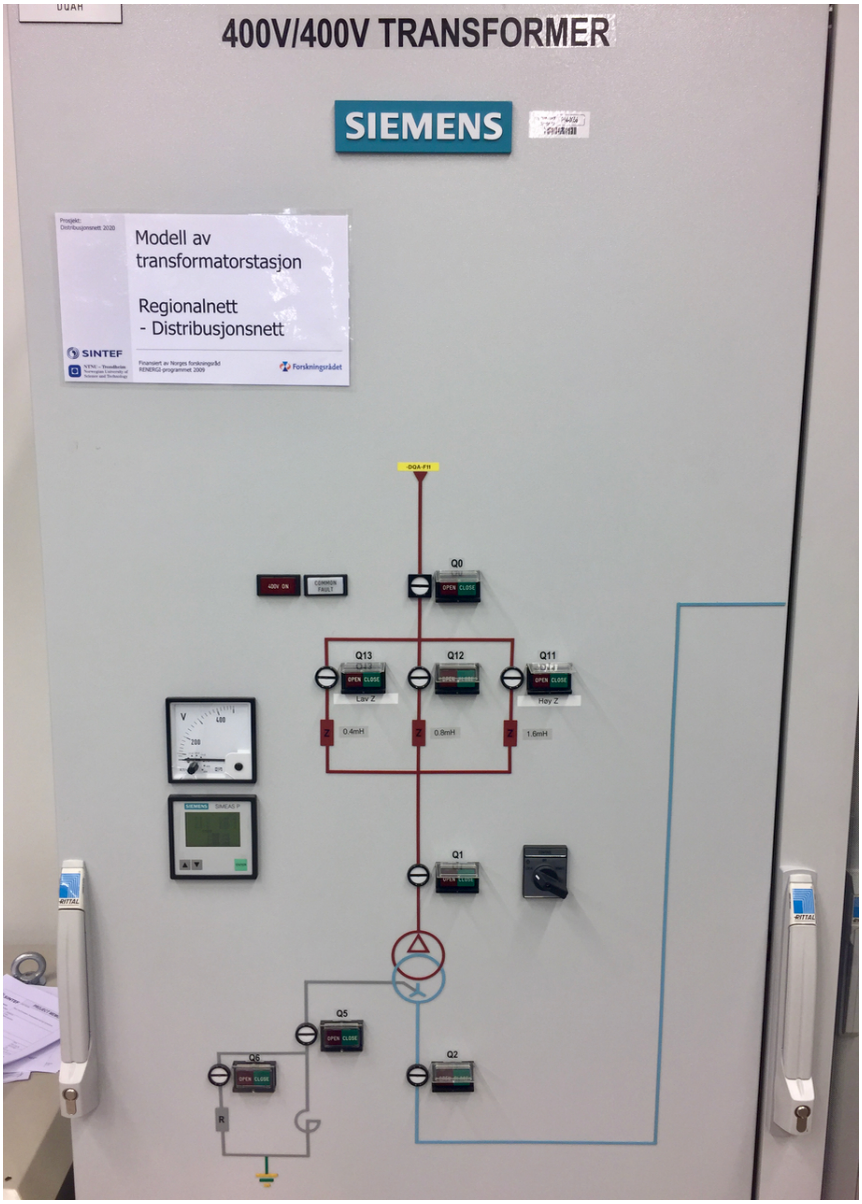


Figure A.3: Substation model.

## A.4 Load

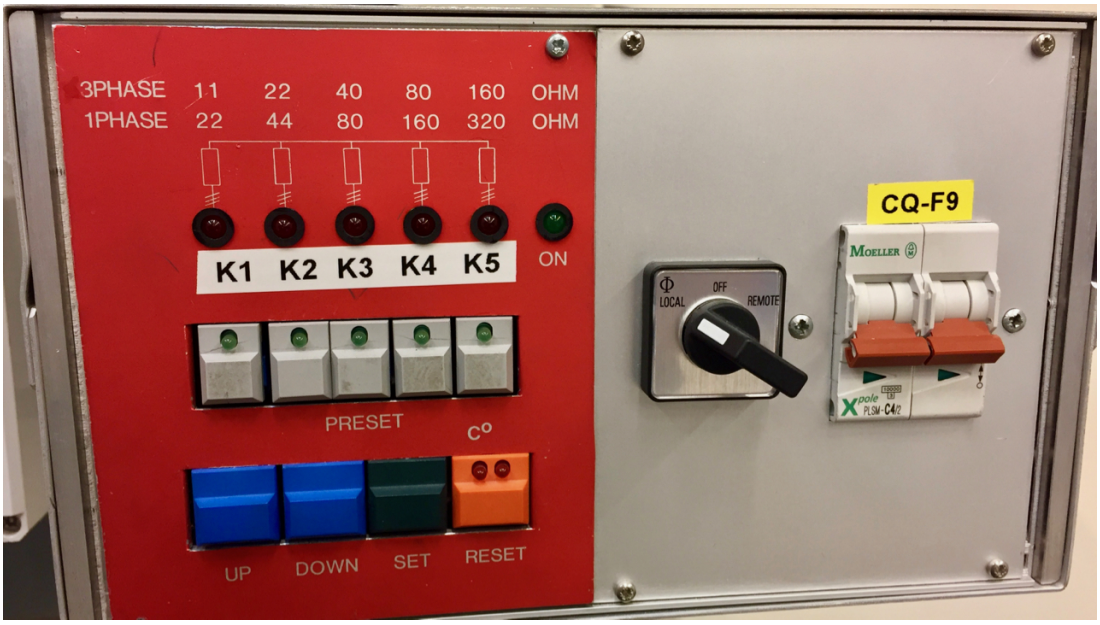


Figure A.4: Load controller.

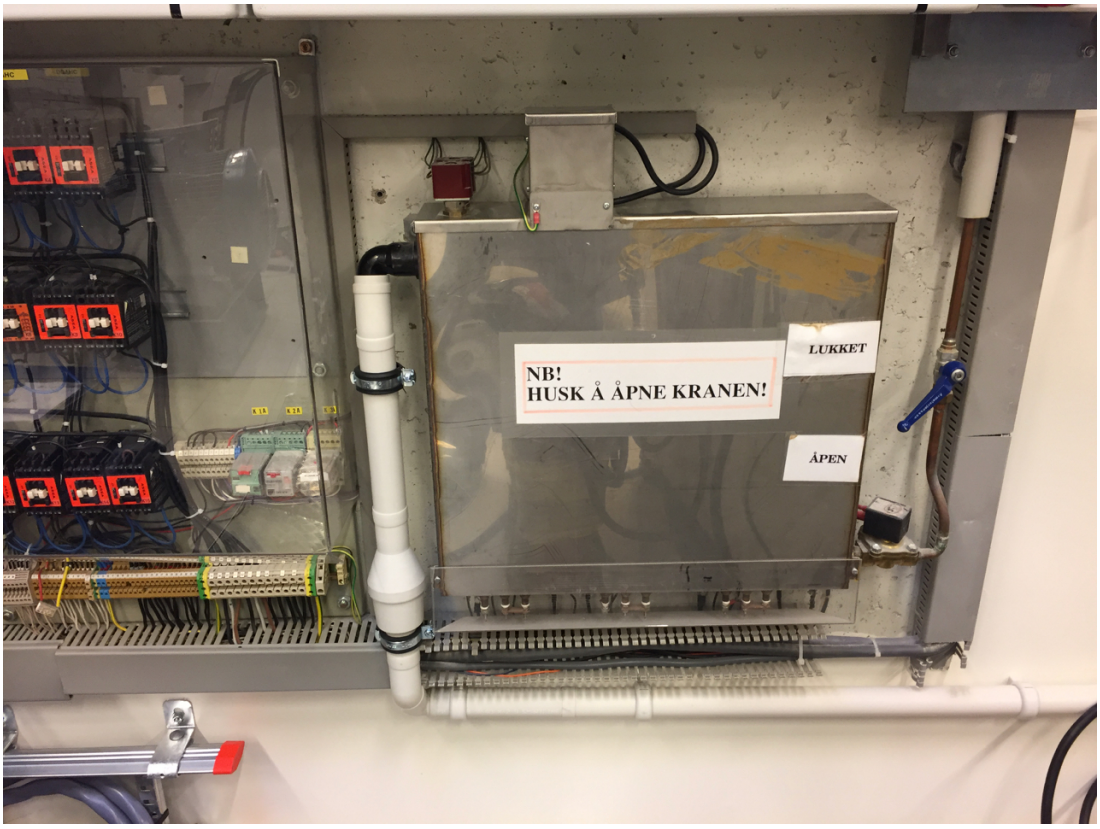


Figure A.5: Water cooled heating element.

Table A.1: Possible load settings

| **Level** | **Coupling** | **Resistance** [Ω] |
|---|---|---|
| 1 | R5 | 160.0 |
| 2 | R4 | 80.0 |
| 3 | R5,R4 | 53.3 |
| 4 | R3 | 40.0 |
| 5 | R3, R5 | 32.0 |
| 6 | R3, R4 | 26.7 |
| 7 | R3, R4, R5 | 22.9 |
| 8 | R2 | 22.0 |
| 9 | R2, R5 | 19.3 |
| 10 | R2, R4 | 17.3 |
| 11 | R2, R4, R5 | 15.6 |
| 12 | R2, R3 | 14.2 |
| 13 | R2, R3, R5 | 13.0 |
| 14 | R2, R3, R4 | 12.1 |
| 15 | R2, R3, R4, R5 | 11.2 |
| 16 | R1 | 11.0 |
| 17 | R1, R5 | 10.3 |
| 18 | R1, R4 | 9.7 |
| 19 | R1, R4, R5 | 9.1 |
| 20 | R1, R3 | 8.6 |
| 21 | R1, R3, R5 | 8.2 |
| 22 | R1, R3, R4 | 7.8 |
| 23 | R1, R3, R4, R5 | 7.4 |
| 24 | R1, R2 | 7.3 |
| 25 | R1, R2, R5 | 7.0 |
| 26 | R1, R2, R4 | 6.7 |
| 27 | R1, R2, R4, R5 | 6.4 |
| 28 | R1, R2, R3 | 6.2 |
| 29 | R1, R2, R3, R5 | 6.0 |
| 30 | R1, R2, R3, R4 | 5.8 |
| 31 | R1, R2, R3, R4, R5 | 5.6 |